Earth-Science Reviews 230 (2022) 104037

Contents lists available at ScienceDirect

Earth-Science Reviews

journal homepage: www.elsevier.com/locate/earscirev

A review on deformation structures of different terranes in the Precambrian Aravalli-Delhi Mobile Belt (ADMB), NW India: Tectonic implications and global correlation

Tapas Kumar Biswal [a,*], Rudra Mohan Pradhan [a], Neeraj Kumar Sharma [a], Sudheer Kumar Tiwari [b], Anouk Beniest [c], Bhuban Mohan Behera [a], Subhash Singh [a], Ragini Saraswati [a], Anamika Bhardwaj [a], B.H. Umasankar [a], Yengkhom Kesorjit Singh [d], Sunayana Sarkar [e], Tanushree Mahadani [a], Gouri Saha [a]

[a] Department of Earth Sciences, IIT Bombay, Powai 400 076, India
[b] Department of Earth Sciences, IIT Roorkee, Uttarakhand 247 667, India
[c] Department of Earth Sciences, Vrije Universiteit Amsterdam, 1081 HV Amsterdam, the Netherlands
[d] Earth, Ocean and Climate Sciences, IIT Bhubaneswar, Odisha 751 013, India
[e] Mukesh Patel School of Technology Management and Engineering, Mumbai 400 056, India

ARTICLE INFO

Keywords:
Aravalli-Delhi Mobile Belt, NW India
Bhilwara Terrane
Aravalli-North Delhi Terrane
Aravalli-South Delhi Terrane
Structural geology
Multiple phases of folding and shearing
Columbia and Gondwanaland Supercontinent

ABSTRACT

The Aravalli-Delhi Mobile Belt (ADMB) in the northwestern part of the Indian Shield represents the final stage of a complex tectonic evolution witnessed by the recognition of three distinct orogenies that have resulted in northwestward accretion of the terranes belonging to Archaean to Neoproterozoic ages. In this contribution, a review of the deformation structures of different terranes is discussed with their tectonic implications and global correlation with other supercontinent assemblies. In the west, the NE-SW trending Neoproterozoic South Delhi terrane is marked by coaxial folding between DF1 and DF2 along the NE-SW axis and cross folded by DF3 folds in the NW-SE axis. Several meso- to large-scale DF2 thrusts and DF4 fractures occur in the belt, that acted as channels for the exhumation of granulite and basement gneisses. Excess shortening led to orogen parallel extension and lateral escape of the material that reactivated the DF2 thrusts as strike-slip faults. Based on the ages of *syn*-DF1 granite gneisses, DF4 fractures, the South Delhi orogeny has been constrained between 0.87 and 0.6 Ga. The Paleoproterozoic North Delhi Terrane is marked by a coaxial folding between NF1 and NF2 folds and later cross-folded by NW-SE trending NF3 folds, producing dome- and basin-structures. Age of syntectonic granite and late-stage metamorphism constrain the north Delhi orogeny between 1.8 and 0.96 Ga. The Paleoproterozoic Aravalli Terrane is divided into a shallow-marine eastern and deeper marine western part by the Rakhabdev suture zone. The entire assemblage of terranes was folded by N*E*-SW isoclinal and recumbent AF1 folds which, with progressive deformation, were reoriented with a *E*-W axial trend. The AF2 is upright and NE-SW trending. The AF3 folds are E-W to NW-SE trending and have produced type 1 and type 2 interference patterns, with AF2 and AF1 respectively. Age of *syn*-AF1 migmatisation in the northern part and syn-AF3 granites in the south constrain the Aravalli orogeny between 1.7 and 0.96 Ga, coeval with the North Delhi orogeny. The granulite and charnockite were tectonically emplaced within the Sandmata Complex during the Aravalli orogeny. The Archean Bhilwara terrane, produced from the Bhilwara orogeny, marks the stabilisation of the crust in NW India by the intrusion of Berach and equivalent granites at 2.6 Ga. The terrane is divided into the Sandmata and Mangalwar complexes that consist of migmatite gneisses with slivers of greenstone. Several Neoarchean to Paleoproterozoic volcano-sedimentary schist belts were tectonically interlaced within the Mangalwar Complex. The migmatitic rocks of the terrane show flow folding in various directions while the schist belts are characterized by extremely appressed N*E*-SW trending reclined folds (BF1 and BF2), inverted BF2 folds, E-W open BF3 folds, and multiple strike-slip shear zones and thrusts. The ADMB exhibits a syntaxial bend in the eastern part attributed to indentation tectonics by Berach granite during *syn*-South Delhi orogeny. The Aravalli orogeny can be correlatable with Nuna orogeny, whereas the South Delhi orogeny can be correlated with the

* Corresponding author.
E-mail address: tkbiswal@iitb.ac.in (T.K. Biswal).

https://doi.org/10.1016/j.earscirev.2022.104037
Received 11 November 2021; Received in revised form 11 April 2022; Accepted 25 April 2022
Available online 2 May 2022

Pan-African orogeny that gave rise to Columbia and Gondwanaland Supercontinent assembly. The Grenville orogeny has experienced thermal rejuvenation in the Aravalli and Bhilwara terranes.

1. Introduction

The Aravalli- Delhi Mobile Belt (ADMB) of the northwestern part of the Indian Shield is a very important geological terrane that preserves rock successions from the Archean to the Cenozoic (Heron, 1953; Sinha-Roy et al., 1998; Roy and Jakhar, 2002), with excellent exposures of outcrops and profiles sections. The belt provides unique opportunities to study the deformation pattern of the rocks which helps in understanding the tectonic process responsible for the creation of the mobile belt. Geochronology of such deformation events constrains the period of orogenies and accretion of different terranes to the mobile belt and aids with correlation of the supercontinent assembly. The ADMB has been studied extensively over the last century with the most important contribution to geological mapping and stratigraphic classification coming from the Geological Survey of India (Coulson, 1933; Gupta, 1934; Heron and Ghosh, 1938; Raja Rao et al., 1971; Sinha-Roy et al., 1998). These studies have been compiled by Heron (1953) and Gupta et al. (1980) (Fig. 1a, b). Heron (1953) described a synclinorium structure for the ADMB with the Archean Banded Gneissic Complex (BGC) as the basement; this was then overlain by Aravalli and Delhi rocks sequentially (Fig. 1c). Gupta et al. (1980, 1997) interpreted lateral accretion of the Aravalli and Delhi terranes to Archean Bhilwara terrane (Fig. 1d); there is an absence of Aravalli or BGC rocks on the western flank of the ADMB. Further, the volcano-sedimentary belts exposed within the BGC at Hindoli, Jahazpur, Pur-Banera, and Rajpura-Dariba, which were previously included in Aravalli Terrane by Heron (1953), were regrouped under the Bhilwara Terrane by Gupta et al. (1997). The Raialo series rocks exposed around Kankroli were grouped under the Aravalli Terrane and those exposed around Ras were grouped under South Delhi Terrane. The concept discussed in Heron (1953) and Gupta et al. (1980) has been intermittently updated with the application of modern structural geology, plate tectonics concept, geochronology, and advanced analytical methods of minerals and rock analysis (Holmes, 1955; Gangopadhyay, 1967; Naha and Chaudhuri, 1968; Crawford, 1970; Naha and Halyburton, 1974, 1977; Synchanthavong and Desai, 1977; Mukhopadhyay and Dasgupta, 1978; Choudhary et al., 1984; Sharma, 1988; Sinha-Roy, 1988; Pandit et al., 2003; Singh et al., 2010; Kaur et al., 2020, 2021; Singh et al., 2021).

In this study, we have reviewed the structural history of different terranes from several published pieces of literature on different parts of the mobile belt and compiled them into a single document. Further, the chapters are organized with an introduction to the geological setting and tectonic evolution of a particular terrane; this is followed by a detailed analysis of deformation structures with stereoplots and profile sections. In the discussion chapter, we have provided possible explanations of the structural framework of the region with its tectonic implications. Further, a brief comparison between the ADMB with Phanerozoic and other Precambrian orogens has been made from a deformation point of view. Based on geochronological data, a correlation has been made with supercontinent assembly. Though extensive metamorphic and geochemistry work has been done on Aravalli orogen, we could not include them as they are beyond the scope of the paper.

2. Terranes of the Aravalli–Delhi mobile belt (ADMB)

ADMB has undergone three distinct orogenies i.e. the Bhilwara orogeny (ca. 2.6 Ga, comparable with Insel orogeny of Antarctica, Anderson, 1999), the Aravalli orogeny (ca. 1.7–0.96 Ga, comparable with Nuna orogeny, Rogers and Santosh, 2002; Zhao et al., 2002), and the South Delhi orogeny (ca. 0.87–0.0.6 Ga, comparable with the early part of Pan-African Orogeny, Singh et al., 2021). The Aravalli and North Delhi orogenies (1.8–1.7 to 0.96 Ga) are coeval. The terranes produced by these orogenies are (from younger to older) the Meso-Neoproterozoic South Delhi terrane, the Paleoproterozoic North Delhi, and Aravalli terranes, and the Archean- Bhilwara terrane (Mangalwar Complex and Sandmata Complex) (Fig. 1b).

2.1. South Delhi Terrane

2.1.1. Geological settings

The Meso-Neoproterozoic South Delhi Terrane (SDT) extends as a NE-SW trending dumb-bell shaped linear belt from Ajmer-Kishangarh in Rajasthan to Ambaji-Khedbrahma in Gujarat (Fig. 1a, Fig. 2). The terrane is characterized by a former passive continental margin with quartzite-pelite-carbonate metasediments intercalated with several bands of synsedimentary rift-related orbicular metarhyolite and pillow-bearing metabasalt. Syn-sedimentary rhyolite flows at Rupnagar (now converted to metarhyolite) show ages of 982 ± 3 Ma (Singh et al., 2010) whereas at Ambaji the reported ages are around 960 Ma (Singh et al., 2021) (Table 1). Volcanogenic sulfide deposits associate with the terrane. As far as the age of rifting and sedimentation are concerned, a previous study on the SDT constrained it at ca. 1.2–0.86 Ga (Singh et al., 2010) and ca. 1.7–1.0 Ga (Wang et al., 2017) (Table 2). Several granite plutons occur within the terrane, some are pretectonic to major deformation and metamorphism (Sendra granite, 967.8 ± 1.2 Ma, Pandit et al., 2003; Pratapgarh granite, 979 ± 33 Ma, Singh et al., 2021; Table 1) some are syntectonic (G1 granite Ambaji area, 860 Ma, G2 (*syn*-DF2) granite, 840 Ma, Singh et al., 2010; Sewariya granite, 878 ± 9 Ma, Singh et al., 2021) and some are latetectonic (G3 granite, 759 ± 6 Ma, Ambaji area, Singh et al., 2010) (Table 1). In the east, the terrane is juxtaposed against the Sandmata Complex (the Archean basement) and the Aravalli Terrane (Paleoproterozoic) along the Kaliguman shear zone (KSZ, Som Thrust to the south, Din and Iqbaluddin, 2000), which is marked by mylonites and extremely stretched conglomerate beds at several places (Srinagar, east of Todgarh, Heron, 1953). KSZ represents a vertical to SW and NW inclined thrust (Heron, 1953; Bhattacharyya et al., 1995; Ruj and Dasgupta, 2014). Klippe remnants of the SDT rocks occur over the Sandmata Complex and the structural fabric in the juxtaposed terranes is disposed at moderate angle to KSZ (Hahn et al., 2020). Further, the Phulad ophiolite belt, representing the remnant of the SDT- ocean, occurs close to KSZ in the west (Khan et al., 2005). Based on these features, KSZ is considered to be the trace of a suture in the subduction zone below the SDT (Sugden et al., 1990; Singh et al., 2010). The western margin of SDT with the basement rocks (Marwar Craton) has been obliterated by the large-scale intrusion of Neoproterozoic granites, the Erinpura granite (863 ± 23 Ma, Just et al., 2011), the Sewariya granite (878 ± 9 Ma, Singh et al., 2021) and the Malani Igneous suite (ca. 771 ± 5 Ma, Gregory et al., 2009) (Table 1). These granites represent arc magmatism. Ras marble (Fig. 2), and rocks of the Sirohi Group at Sirohi and Sojat occur as large-scale rafts within these granites. Late-stage extension produced intra-arc basins over the granite basement at Punagarh, Sindreth, and Marwar between 0.7 and 0.6 Ga (Bhardwaj, 2019). The Phulad thrust (Phulad shear zone- PSZ, Fig. 2), which was once considered to be the western margin of SDT (Heron, 1953), is interpreted as an intra- terrane thrust (Sen, 1980; Singh et al., 2021). A linear belt of the basal conglomerate of South Delhi rocks occurs along the Phulad thrust near Babra and Bar area. Basement rocks belonging to the Sandmata Complex are exposed near Ajmer (1849 ± 8 Ma, Anasagar gneisses, Mukhopadhyay et al., 2000) and Beawar (1614 ± 10 Ma, Beawar gneisses, Kaur et al., 2020) as thrust slices. Bands of 1434 ± 0.6 Ma old pre-Delhi pelitic granulite with a 1085 Ma thermal overprint are exposed at Pilwa-Chinwali (Fig. 1b, west of Ajmer,

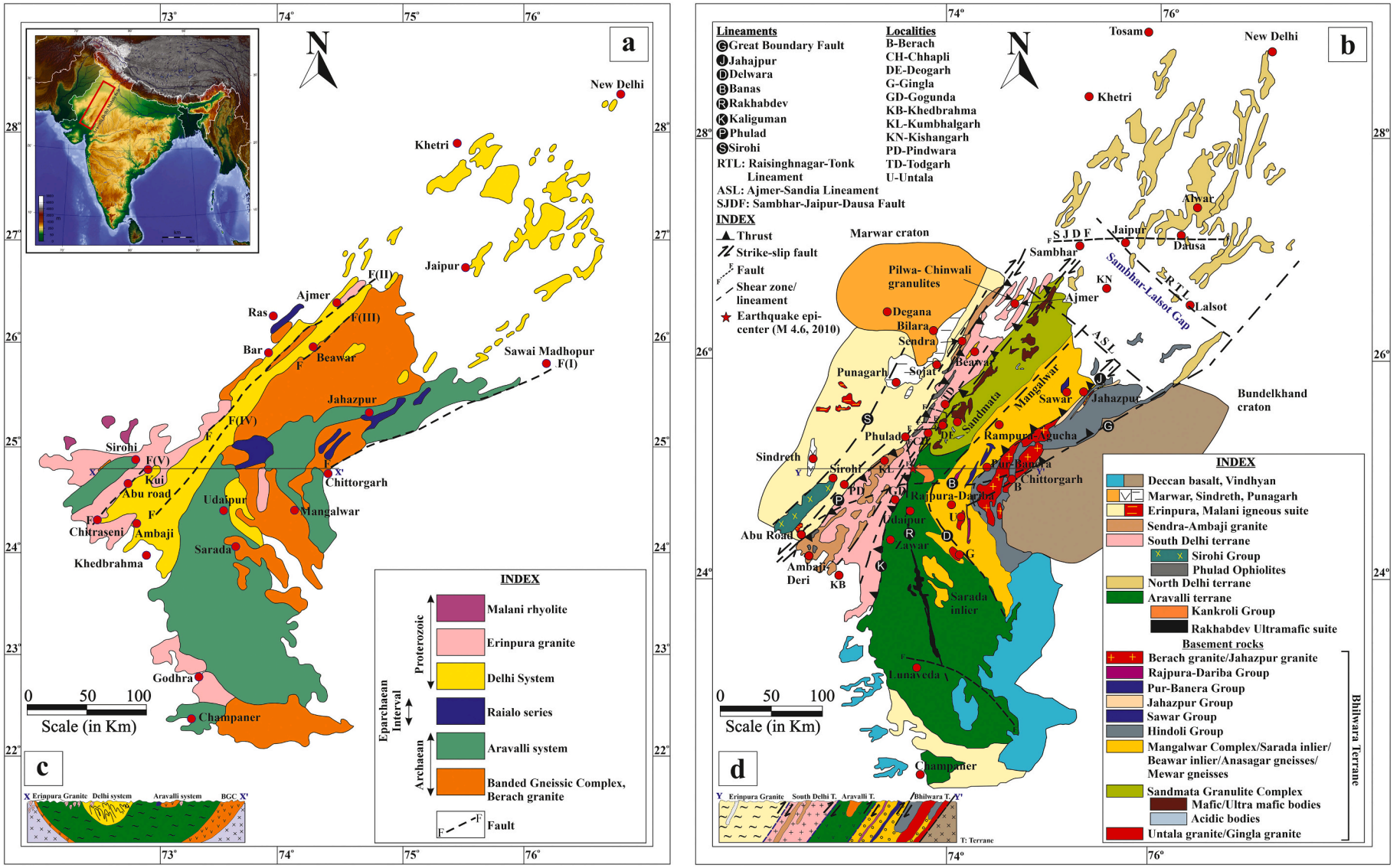

Fig. 1. Geological map of the ADMB (a) after Heron (1953) and (b) after Gupta et al. (1980), redrawn from Singh et al., 2010. Fig. 1c and d are the respective cross-sections of Fig. 1a and b. Fig. 1a inset (Source: https://commons.wikimedia.org/).

Fareeduddin et al., 1994; Bhowmik et al., 2018; Singh et al., 2020, 2021). Based on the age of the syntectonic granites, the South Delhi orogeny is constrained between 0.87 and 0.6 Ga (Table 2), which is similar to the early part of the Pan-African orogeny that gave rise to Gondwanaland Supercontinent.

2.1.2. Small scale structures

The SDT has undergone multiple phases of folding and shearing. The first folding phase was due to buckling with bedding parallel sub-horizontal simple shear deformation. Minor undulations in the bedding produced isoclinal recumbent folds along the NE-SW axis, the DF1 folds (Fig. 3a) (Naha et al., 1984, 1987; Biswal, 1988; Singh et al., 2010; Singh et al., 2021). The folds are extremely flattened and associated with layer parallel stretching, formation of floating hinges, boudinaged folds, and compositional boudins due to the high amount of homogeneous strain. Syntectonic metamorphism during DF1 gave rise to the first schistosity phase (DS1), axial planar schistosity, which is marked by the formation of biotite and hornblende minerals (Babra area, Singh et al., 2021) and at places by granulite-facies minerals such as sillimanite, cordierite, garnet, and spinel (Ambaji area, Singh et al., 2010; Prakash et al., 2021). This suggests that the DF1 metamorphic event occurred over a broad pressure and temperature range, from greenschist to granulite facies metamorphic grade (Fig. 3b). Further, based on the coplanar nature of the magmatic fabric and SF1 fabric in the Sewariya granite and the *syn*-DF1 character of the migmatites associated with the Ambaji granite, the DF1 is constrained at 875–860 Ma, which is now the suggested age for peak metamorphism of the South Delhi orogeny (Singh et al., 2010; Tiwari and Biswal, 2019; Singh et al., 2021). The DF1 folds are involved in coaxial folding with the second folding phase (DF2) producing a type 3 interference pattern. Thus, the DF1 folds have assumed inclined and upright orientation in the limb region of the DF2 fold. The DF2 folds are open in most instances except for a few cases where they are tight to isoclinal. These are upright and show great variation in the wavelength-to-amplitude ratio depending on the competence contrast between the layers involved in the folding (Fig. 3c). The folds are Class 1B type and converted to Class 1C type in response to continuous homogenous strain. Crenulation cleavages (DS2, Fig. 3d) and shear planes developed parallel to the axial plane of such crenulation during this phase. In the greenschist to amphibolite facies rocks, biotite and hornblende are recrystallized along the SF2 fabric while second stage garnet, sillimanite and spinel have grown at the hinge zone of DF2 folds in granulites. This provides evidence that the DF2 folds occurred under the same metamorphic condition as DF1. In a few places near Bar and Babra, the DF1 fold axis trends in the E-W direction (Biswal, 1993), and the fold-axis rotates around the hinge of the NE-SW trending DF2 folds. The DF3 folds have a NW-SE oriented fold-axis trend and in most cases, the

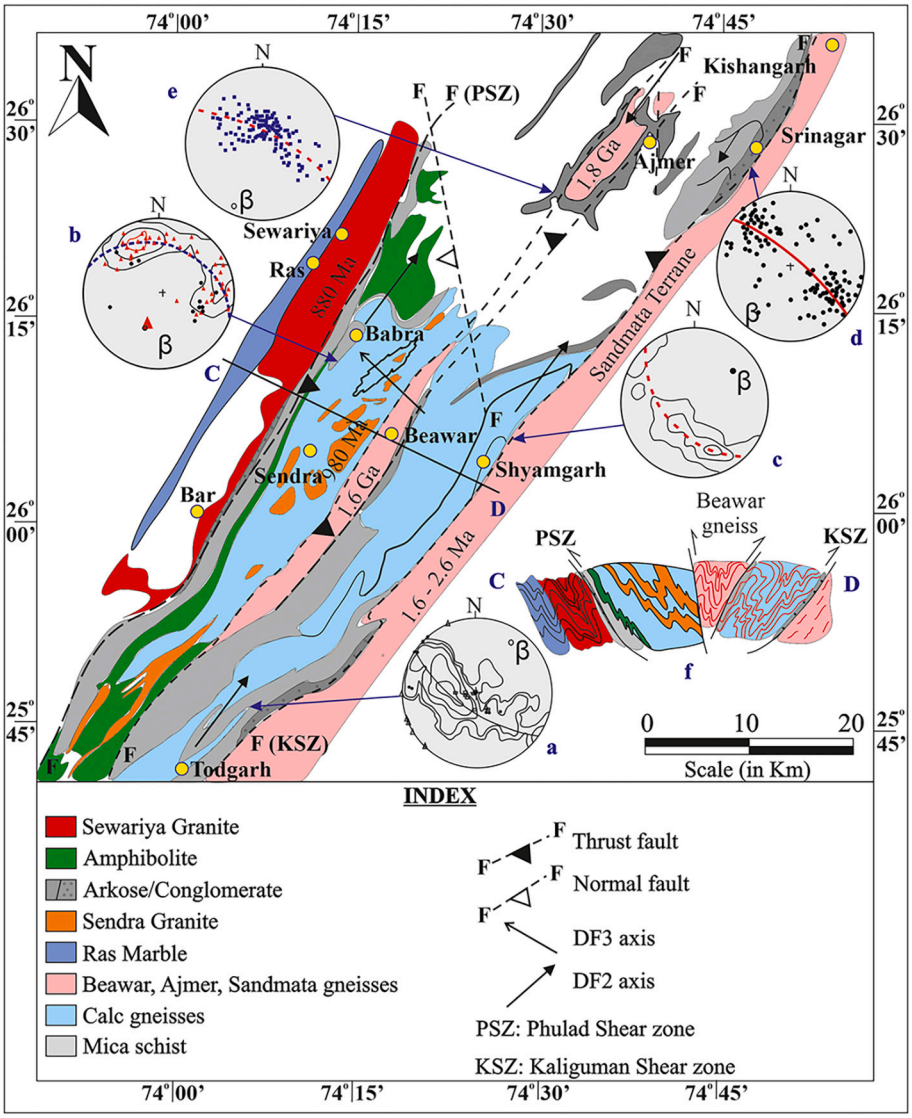

Fig. 2. Geological map of the SDT, drawn after Heron (1953) (a) Stereoplot of DS1 schistosity in Todgarh area, contour pattern indicate distribution over a girdle, interpreting northeasterly plunge of the DF2 axis (β) (Naha et al., 1987), (b) Stereoplot of DS1 schistosity in the Babra area, contour pattern shows distribution over a girdle, interpreting southwesterly plunge of the DF2 axis (β) (Singh et al., 2021), (c) Stereoplot of DS1 schistosity in the Shyamgarh area, contour pattern indicates distribution over a girdle, interpreting NE-ly plunge of the DF2 axis (β) (Bhattacharyya et al., 1995), (d) Stereoplot of DS1 schistosity in the Srinagar area, contour pattern indicates distribution over a girdle, interpreting southwesterly plunge of the DF2 axis (β) (Ruj and Dasgupta, 2014), (e) Stereoplot of DS1 schistosity near the Ajmer area, they show the distribution over a girdle, indicating SW-ly plunge of the DF2 axis (β) (Mukhopadhyay et al., 2010), (f) Cross-section CD, shows oppositely dipping lithological units. Beawar gneiss forms the central line of such divergent thrust sheets. The thrust that appears in the NW block have an NW vergence and the thrusts in the SE block have a SE vergence, representing retro- wedge and pro- wedge thrusts respectively in a collision zone (Singh et al., 2021). The thrusts are overprinted by late-stage strike-slip shearing due to the lateral flow of the material.

Table 1
Geochronological ages of different parts of Aravalli Delhi Mobile Belt (ADMB), NW India.

Formation/Rock-type	Age		Method	Reference
	Million years (Ma)	Billion years (Ga)		
Untala granite	3500 Ma	3.5 Ga	Sm-Nd isochron age	MacDougall et al. (1983)
Mewar gneiss, Amphibolite	3281 ± 3 Ma	3.2 Ga	Zircon age	Wiedenbeck and Goswami (1994)
Rakhiawal gneiss, Northeast of Udaipur	3232.3 ± 0.2 Ma	3.2 Ga	Single zircon evaporation age	Roy et al. (2001)
Darwal granite	2905 ± 0.3 Ma	2.9 Ga	Zircon age	Roy et al. (2012)
Berach granite	2610 ± 50 Ma	2.6 Ga	U-Pb Zircon	Sivaraman and Odom (1982)
Nagar granite, Sandmata	2548 ± 6 Ma	2.6 Ga	Zircon age	Kaur et al. (2021)
Jahazpur granite	2538 ± 5 Ma	2.5 Ga	Zircon age	Dey et al. (2019)
Malola granite, Pur Banera	2538 ± 11 Ma	2.5 Ga	Zircon age	D'Souza et al. (2020)
Jhiri granite North Delhi	2529 ± 6 Ma	2.5 Ga	Zircon age	Misra et al. (2020)
Aravalli craton	2500–2150 Ma	2.0 Ga	Paleosol	De Wall et al. (2012)
Kalalikhera granite, Pur-Banera	2110–2285 Ma	2.1 Ga	Monazite age	Chander et al. (2021)
Ahar River granite, Aravalli	2026 ± 54 Ma	2.0 Ga	Rb-Sr isochron age	Wiedenbeck and Goswami (1994)
Amet granite, Aravalli	1870 ± 200 Ma	1.8 Ga	Rb-Sr isochron age	Choudhary et al. (1984)
Rhyodacite, Hindoli	1854 ± 7 Ma	1.8 Ga	Zircon age	Deb et al. (2002)
North Delhi Terrane, Jasrapura granites	1821.7 ± 0.4 Ma	1.8 Ga	Zircon age	Kaur et al. (2009)
Anasagar granite gneisses	1849 ± 8 Ma	1.8 Ga	Single zircon evapo.age	Mukhopadhyay et al. (2000)
North Delhi Terrane arc magmatism	1820 Ma	1.8 Ga	Zircon age	Kaur et al. (2013, 2017)
Sandmata granulite intrusion and granulite facies metamorphism	1723 ± 14 Ma	1.7 Ga	Zircon age	Sarkar et al. (1989)
Gothra granite, North Delhi Terrane	1691 ± 4 Ma	1.7 Ga	Zircon age	Knight et al. (2002)
Sandmata granulite metamorphism and shearing	1621.7 Ma	1.6 Ga	Zircon age	Roy et al. (2012)
Age of South Delhi sediments	1740 ± 39 Ma to 1091 ± 43 Ma	1.7 to 1.0 Ga	Zircon age	Wang et al. (2017)
Beawar gneiss	1614 ± 10 Ma	1.6 Ga	Zircon age	Kaur et al. (2020)
Kishangarh nepheline syenite	1490 ± 150 Ma	1.5 Ga	Rb-Sr age	Crawford (1970)
Kishangarh nepheline syenite	1438 ± 15 Ma	1.4 Ga	Zircon age	Kaur et al. (2021)
Pelitic granulites, Pilwa-Chinwali	1434 ± 0.6 Ma	1.4 Ga	Single zircon evaporation age	Fareeduddin (1998)
Pelitic granulites, Pilwa-Chinwali	1085 Ma	1.0 Ga	Monazite age	Bhowmik et al. (2018)
Rupnagar metarhyolite	982 ± 3 Ma	0.98 Ga	SHRIMP zircon age	Singh et al. (2021)
Pratapgarh granite	979 ± 33 Ma	0.98 Ga	SHRIMP zircon age	Singh et al. (2021)
Sendra granite	967.8 ± 1.2 Ma	0.96 Ga	Pb/Pb age	Pandit et al. (2003)
Godhra granite, Aravalli Terrane	965 ± 40 Ma	0.96 Ga	Rb-Sr age	Gopalan et al. (1979)
Metarhyolite in Ambaji granulite SDT	960 Ma	0.96 Ga	SHRIMP zircon age	Singh et al. (2010)
Khetri-Nawa belt	1100 ± 20 Ma to 950 ± 16 Ma	1.1.to 0.96 Ga	Monazite age	Pant et al. (2008)
South Delhi deformation and metamorphism	875–650 Ma	0.87 to 0.65 Ga	Monazite age	Tiwari and Biswal (2019)
Sewariya granite, SDT	878 ± 9 Ma	0.87 Ga	SHRIMP zircon age	Singh et al. (2021)
SDT DF1 folding metamoprhism, Babra	864 Ma	0.86 Ga	Monazite age	Singh et al. (2021)
Erinpura granite	863 ± 23 Ma	0.86 Ga	Monazite age	Just et al. (2011)
Granulite metamorphism and anatexis in Ambaji granulite SDT, G1 granite	861 ± 83 Ma	0.86 Ga	SHRIMP zircon age	Singh et al. (2010)
G2 granite intrusion to Ambaji granulite SDT	842 ± 19 Ma	0.84 Ga	SHRIMP zircon age	Singh et al. (2010)
SDT DF2 folding and shearing, Babra	811–718 Ma	0.8 Ga	Monazite age	Singh et al. (2021)
Malani igneous suite	771 ± 5 Ma	0.77 Ga	U-Pb and 40Ar/39Ar	Gregory et al. (2009)
Microgranite intrusion, Ambaji G3	759 ± 6 Ma	0.76 Ga	SHRIMP zircon age	Singh et al. (2010)
Punagarh basin sedimentation	771–655 ± 3 Ma	0.6 Ga	Ar-Ar age	Bhardwaj (2019)
SDT DF4 brittle shearing, Babra	588 Ma	0.6 Ga	Monazite age	Singh et al. (2021)

direction of motion was in the vertical plane (Fig. 3e). Hence superimposition of DF3 on DF2 has produced dome- and basin- structures (Fig. 3f). With the recumbent DF1 folds, a mirror-image pattern is produced. The DF1-DF2 axes show folding by DF3 folds and hence their axes show dispersion in orientation all through the terrane. Axial planar crenulation cleavage and shear fractures are associated with DF3 folding (Fig. 3e). The G3 granite is syntectonic with DF3 folding. Several brittle fractures and faults (DF4) have affected the SDT and monazite geochronology constrains the DF4 event at 0.65 Ga that defines the end of the South Delhi orogeny. Thus, the South Delhi orogeny is bracketed between 0.87 and 0.6 Ga, correlatable with the early part of the Pan-African orogeny. The Pan-African orogeny has been divided into two parts, namely ca. 900–630 Ma which is characterized by terrane accretion as seen in the Arabian-Nubian shield, and 630–540 Ma, which shows collision- and escape-tectonics in many parts of East African orogen (Rogers and Santosh, 2002; Kröner and Stern, 2005; Rino et al., 2008).

2.1.3. *The large-scale structures*

In the Ajmer and Kishangarh area, SDT is marked by several NE-SW trending parallel ridges made of arkose and marble. The strike of those

Table 2
Comparison of orogenic events in different terranes of the ADMB, NW India.

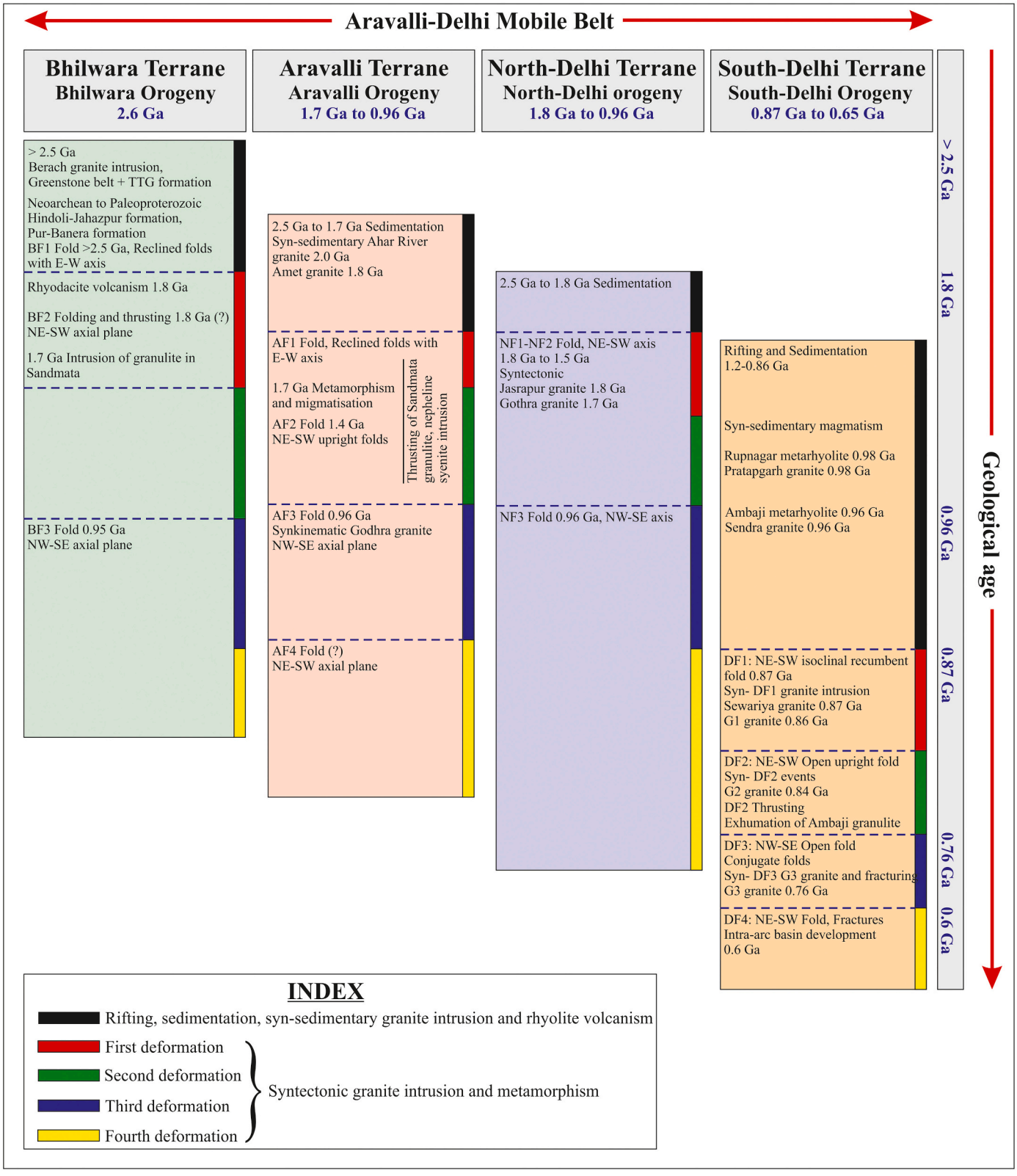

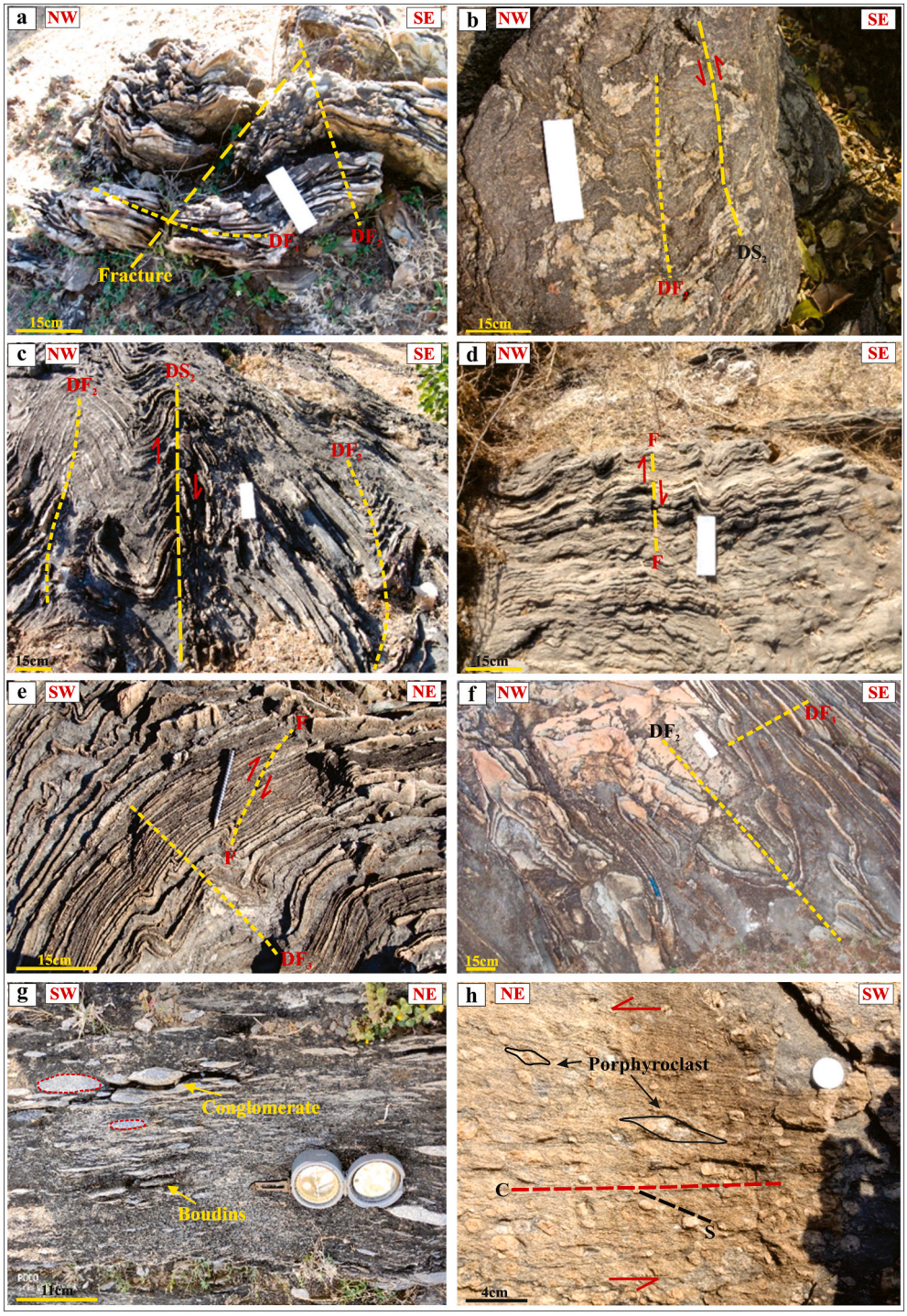

Fig. 3. Structures of the South Delhi Terrane (Singh et al., 2010, 2021; Tiwari et al., 2020a) (a) Coaxial folding between DF1 and DF2, vertical section, looking towards the NE, (b) Migmatite from the Ambaji area, showing DF2 folding and DS2 shear, vertical section, looking towards the NE, (c) DF2 fold showing axial plane shear, vertical section, looking towards the NE, (d) DS2 crenulation cleavage, vertical section, looking towards the NE, (e) DF3 fold with axial plane shear, horizontal section, looking towards the NW, (f) Dome- and- basin structure, horizontal section, looking towards the NE, (g) Conglomerate from Bar area, horizontal section, looking towards the NW The quartzite layers show a boudin structure, (h) Mylonite with sigmoidal porphyroclasts and S—C fabric, horizontal section, looking towards the SE.

ridges represents the DS0/DS1 fabric on the limb portion of the large scale DF2 fold (Fig. 1a, Fig. 2). To the south of Ajmer, the SDT displays a continuous outcrop of calc schist/gneiss, amphibolite, metarhyolite, and mica schist at Babra, Bar, Beawar, Shyamgarh, and Todgarh areas (Fig. 2). In most instances, the DF1 folds occur on a small scale (cm to m). Mappable DF1 folds occur near Todgarh where the mica schist and calc gneiss show a DF1 antiform and the DS1 schistosity cross-cut the DS0 beds at the hinge zone of the fold. The DF1 fold is refolded by the NE-SW trending DF2 fold producing a large-scale type 3 interference pattern. The stereoplot of the DS1 fabric shows a girdle distribution with the β- axis plunging to the NE (Fig. 2a, Naha et al., 1987). A similar pattern is produced by the metarhyolite band within the calc- schist near Beawar (Singh et al., 2020, 2021). The metarhyolite represents rift-related volcanic flow that was deposited along with other sedimentary rocks in the South Delhi basin and has been dated to be ca. 980 Ma (Singh et al., 2021). The metarhyolite along with surrounding calc-schist has suffered DF1 folding followed by, DF2 folding resulting in a large-scale type 3 interference pattern. In contrast to the DF1 folds, large-scale DF2 and DF3 folds are abundant in the terrane, which has produced mappable-dimension antiforms and synforms. Interference between DF2 and DF3 folds resulted in large-scale domes. Near Babra there are several domal outcrops described by amphibolite-mica schist and calc-schist bands. Many of these domes have a granitic core e.g. the Pratapgarh granite near Babra. These domal outcrops formed when NE-

SW directed compression during DF3 folding superimposed the NE-SW axial trending DF2 folds (Fig. 2). The DF2 fold has been converted to plane-noncylindrical geometry. The stereoplot of DS1 foliation indicates girdle distribution with a β-axis plunging to SW, parallel to the DF2 trend (Fig. 2b, Singh et al., 2021). The Sewariya granite batholith is characterized by a tectonomagmatic foliation that is oriented parallel to the DS1 schistosity. The granite along with the Ras marble and mica schist has been folded by the DF2 folds. The calc gneiss-arkose bands close to the eastern margin of the terrane describe a northeasterly plunging anticline near Shyamgarh (Bhattacharyya et al., 1995) and southwesterly plunging syncline at Srinagar (Ruj and Dasgupta, 2014). The DS1 foliation describes girdle distribution suggesting the folds belong to the DF2 generation (Fig. 2c,d). Near Ajmer, Anasagar granite gneiss occurs within a DF2 antiformal core. The stereoplot shows a plunging β-axis roughly towards SW (Fig. 2e, Mukhopadhyay et al., 2010). The eastern contact zone between the gneiss and the cover rock is a zone of dislocation and is marked by a southeasterly verging fold-thrust belt, while the western contact zone shows mylonites that verge towards the northwest. A complimentary synform is present near Ajmer. The profile across the SDT (CD, Fig. 2f) shows a large scale synform similar to what Heron (1953) mapped as the Delhi synclinorium. The Beawar gneiss occurs at the core of the synform, being bounded by oppositely dipping conjugate thrusts. The Beawar gneiss represents the basement rocks that have been sliced up and popped up between these conjugate thrusts. The Beawar synclinal axis merges with Ajmer synclinal axis to the north (Gupta et al., 1997).

2.1.4. Shear zones

The NE-SW striking KSZ and PSZ represent large-scale DS2 thrusts. The PSZ is marked by SE-dipping mylonitic foliation with down-dip stretching lineations. Kinematic indicators include mantled porphyroclasts, S—C cleavage, and asymmetric folds, point to a NW vergence for the PSZ. The Bar-Babra conglomerates occur along the PSZ and are extremely stretched down-dip, by shearing (Fig. 3g). The DF1 and DF2 folds have been converted to sheath folds due to heterogeneous shear along the thrust (Sengupta and Ghosh, 2004). Strain analysis indicates two stages of shearing, first by thrusting in NW direction and later by dextral strike-slip shearing (Dasgupta et al., 2012). Strike-slip shearing has created low-angle plunging stretching lineation that overprinted the down-dip lineation. The conglomerates were rotated in a clockwise manner on the horizontal surface during dextral shearing. The Sewariya granite pluton lying west of the PSZ is marked by DF2 shear zones and mylonites. In the eastern part of the terrane margin, the KSZ is marked by a SW-verging thrust near Srinagar (Ruj and Dasgupta, 2014), while near Shyamgarh, the thrust is either vertical or steeply verging towards the NW (Bhattacharyya et al., 1995). The thrust is marked by mylonitic foliation with down-dip stretching lineations. The basal conglomerate near Srinagar and north of Todgarh have been sheared along the thrust. The folds were converted to sheath folds with down-dip stretching. This was followed by the second stage of dextral shearing that produced horizontal stretching lineations and clockwise rotation of conglomerate in the horizontal plane. The DF2 folds near Shyamgarh have been sheared on its eastern limb by strike-slip shearing. Further, the conjugate thrusts near Beawar and Anasagar have tectonically emplaced the pre-Delhi granite gneisses such as Beawar gneiss and Anasagar gneiss into the SDT. Fold-and-thrusts belts developed in the Ajmer area involving the basement gneisses and cover rocks (Mukhopadhyay et al., 2010). In addition to thrusts, an N-S striking normal fault to the east of Babra and Beawar has displaced the western block downward (Fig. 2). As a result, the eastern block stands out, ensuing the basement rocks (Anasagar gneisses) and granulites (Pilwa-Chinwali) (Singh et al., 2021) exposed due to erosion.

2.1.5. Central SDT

The central part of SDT, from south of Todgarh to Kumbhalgarh, has attained the narrowest width (Fig. 1b) and is marked by several large-scale NE-SW trending DF2 antiforms and synforms (Kamlighat and Goramghat areas, Gupta et al., 1997) with the PSZ and KSZ continuing further south. Within these shear zones, the fold axis of small-scale DF1 and DF2 folds are reoriented to the NW-SE direction parallel to the direction of slip due to inhomogeneous shear (Choudhury et al., 2016; Hatui and Chattopadhyay, 2020). *E*-W directed late-stage strike-slip faults cross-cut the entire width of SDT, at Todgarh, Deogarh, Chhapli, Gogunda, etc. (Gupta et al., 1997). The Banas shear zone extends westward and merges with one of those strike-slip faults running through Gogunda (Fig. 1b). Further, rare WNW- striking faults forming a conjugate pair with the above set of faults occur in the belt. Taking the acute angle between them in the brittle deformation regime, the compressive stress is determined to be directed in the NW-SE direction. The WNW-oriented faults are reactivated causing seismicity, inducing neotectonics activity in the region (Kumar and Pandit, 2020). Beyond Kumbhalgarh, towards the south, the SDT has acquired a larger width and the Aravalli Terrane is juxtaposed against SDT. The overall geometry of the SDT resembles a dumbbell-shaped belt with wider parts in NE and SW and a narrower part at the centre. This shape can be explained by a higher concentration of strain at the centre that led to the lateral extrusion of material, exemplifying escape tectonics, which will be discussed in chapter 3.5 later.

2.1.6. Southwestern SDT

The Pindwara, Khedbrahma, and Ambaji areas constitute of some major tectonic blocks in the southwestern part of the SDT (Fig. 1b). The Pindwara area notices coaxial folding in NE-SW direction and shearing along the DF2 axial plane (Dutta et al., 2021). The Khedbrahma area is occupied by schists and quartzite that are coaxially folded along a NE-SW axis and cross folded in the NW-SE axis; the interference has given rise to the dome- and basin-structures on a large- scale (Prakash et al., 2012). The Ambaji area is located in the far SW part of the SDT and is unique in terms of having preserved granulite facies rocks including pelitic-, calc- and mafic granulites (Desai et al., 1978; Biswal et al., 1998a, 1998b; Fig. 4). Granulite occurs in a tectonically exhumed block, surrounded by low-grade rocks having been separated by shear zones. The deformation pattern in low-grade rocks and the granulite is comparable and matches with that of other parts of SDT (Biswal, 1988; Biswal et al., 1998a, 1998b; Biswal et al., 2004; Singh et al., 2010; Mahadani et al., 2015). The DF1 folds are recumbent and isoclinal and formed syntectonically with the granulite facies metamorphism and migmatisation in the granulite (Fig. 3b). The first granites (G1) were produced and emplaced in the melting process. The DF2 phase is coaxial with DF1 in the N*E*-SW axis and DF2 is associated with the second granite (G2) intrusion and formation of axial planar shear zones (Fig. 3b). These shear zones show an imprint of thrust tectonics at a higher temperature, which is subsequently overprinted by sinistral strike-slip tectonics at low temperatures. Thrusting followed by intrusion of granitic magma and the formation of a positive flower structure due to the splay of strike-slip faults created channel flow for the exhumation of the granulite. Sigma and delta porphyroclasts, S—C fabric, and asymmetric folds (Fig. 3h) are shear kinematic indicators (Ramsay and Huber, 1987) observed in the shear zones. Vorticity analysis of the porphyroclasts points towards transpressive strain (low kinematic vorticity number, Ghosh and Ramberg, 1976; Passchier, 1987) during high-temperature thrusting and simple shear-dominated strain during low-temperature strike-slip shearing (high kinematic vorticity number, Tiwari et al., 2020a). Large-scale pseudotachylite and deformed pseudotachylite veins have intruded during the DF2 shearing event (Biswal et al., 2004; Sarkar and Biswal, 2005; Tiwari and Biswal, 2019). The third deformation phase (DF3) occurred in an NW-SE direction and is associated with E-W, ESE-WNW strike-slip shearing that moved the material in the horizontal plane during the folding. As a result, large-scale DF3 folds have E-W oriented limbs, and the lithological units, as well as the DF2 fold axial plane and axis, are now reoriented from NE-SW to E-W direction on that limb (Fig. 4). The interference between

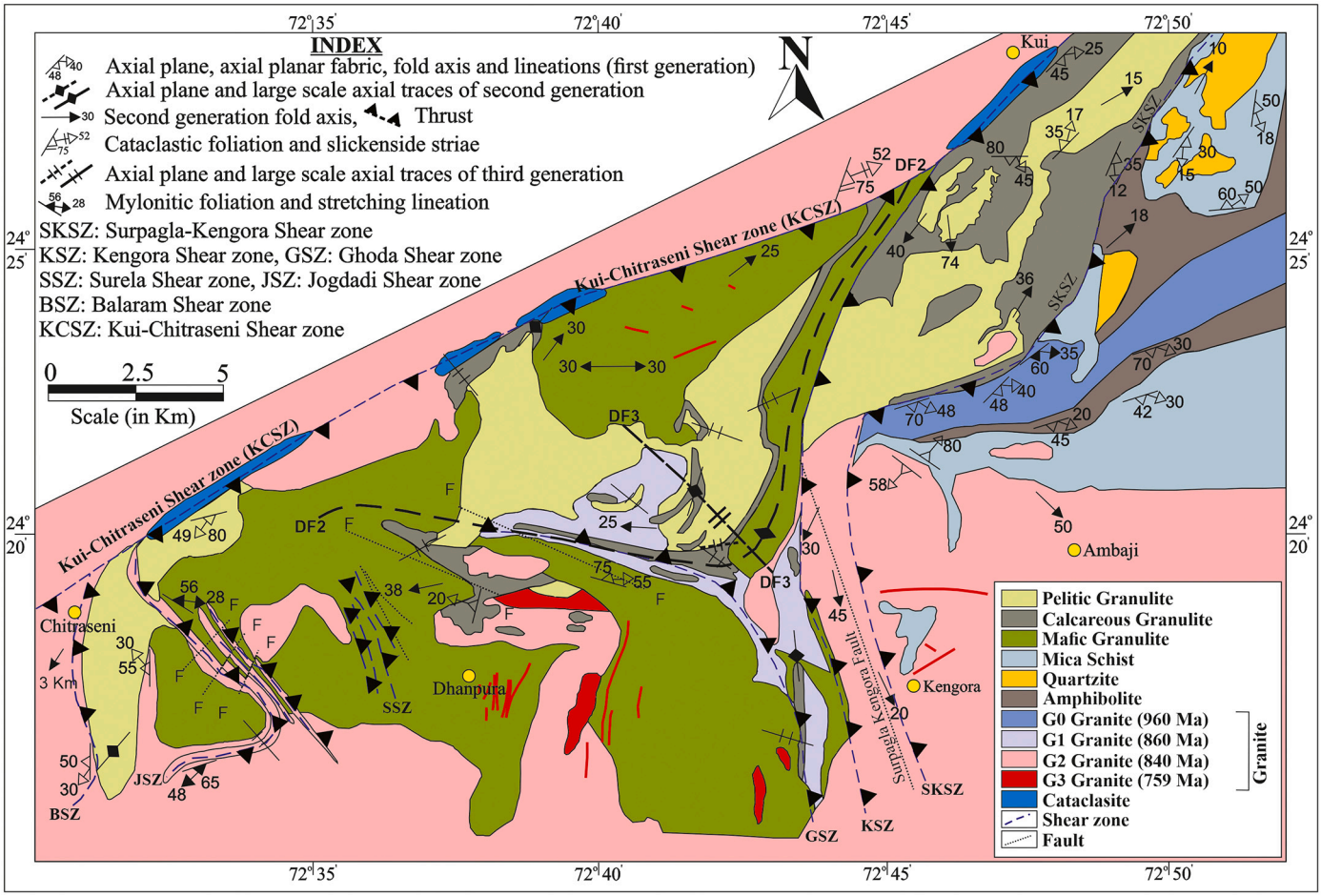

Fig. 4. Geological map of the Ambaji area, South Delhi Terrane, drawn after Singh et al. (2010). The DF2 axial plane rotates around the DF3 hinge.

DF2 and DF3 folds has produced a mirror-image pattern. G3 granites intruded along fractures parallel to DF3 folds. There are folds from a fourth deformation phase (DF4) with fold axes oriented in the NE-SW direction that has produced dome- and basin-structures with DF2 folds (Biswal, 1988; Singh et al., 2010). The area is marked by late-stage strike-slip and normal faults in NE-SW and ESE-WNW directions. A paleostress analysis of those faults indicates that NW-SE-directed extensional tectonics affected the region during brittle deformation (Tiwari et al., 2020b). During brittle deformation, previous shear zones have been reactivated as normal faults, for example, the Kui-Chitraseni and Surpagla-Kengora faults. Normal faulting aided by erosion eventually unroofed the granulites to the surface. These faults and fractures have served as the pathways for mineral-rich fluids to percolate into the low-grade schistose rocks (< 0.76 Ga) giving rise to hydrothermal Cu, Pb, and Zn mineralization (Sharma and Biswal, 2020; Sharma et al., 2022) and U mineralization in the albitite veins (Ray, 1987). Further, the fractures acted as suitable waterways for aquifers (Pradhan et al., 2021, 2022).

2.1.6.1. Sirohi Group. Isolated metasedimentary outcrops within the granitic country, around Sirohi and Sojat, show a similarity in deformation history to SDT (Fig. 1b). The NE-SW folding followed by thrusting and dextral strike-slip shear mark the deformation history of the Sirohi Group (De Wall et al., 2014). The DF1 folds are isoclinal and recumbent with a NE-SW trending fold axis. These folds are involved in coaxial folding with DF2, which results in open and upright type 3 interference patterns. The DF2 folds are associated with NW verging thrust faults. DF3 is oriented in the NW-SE direction and has formed crenulation cleavage (Roy and Sharma, 1999). Several N-S trending large-scale extensional fractures and grabens occur in the belt. and some of the large-scale fractures host the Malani Igneous suite of rocks (Sharma, 2005). N-S trending Punagarh and Sindreth volcano-sedimentary basins formed in those grabens over the granitic basement. The Punagarh basin is cross-cut by a conjugate set of strike-slip faults indicating compression in the *E*-W direction that led to an inversion of the basin (Bhardwaj and Biswal, 2019).

2.2. North Delhi Terrane

2.2.1. Geological settings

The Paleoproterozoic North Delhi Terrane (NDT) is located in the northeastern part of the Aravalli orogen (Fig. 1a, b). The terrane is widely spread out across the width of the entire orogen in the form of isolated ridges of quartzite and calc-schist overlying the Archean gneissic basement. Several hogbacks occur within a vast tract of alluvium at Nawa, Alwar, and south of Delhi (Fig. 5). The southern continuity of the NDT to other terranes of the ADMB is broken due to the Sambhar-Lalsot geomorphologic break marked by a vast tract of alluvium. Sambhar-Jaipur-Dausa strike-slip fault (Sinha-Roy, 2004), the Ajmer-Sandia lineament, and the Raisingnagar-Tonk lineament (Bakliwal and Ramasamy, 1987) are some of the structural grains in the geomorphologic gap.

The NDT is divided into three NE-SW trending sub-basins namely the Khetri- Nawa, Alwar-Jaipur, and Bayana-Lalsot sub-basins. These sub-basins comprise the Raialo, Alwar, and Ajabgarh groups of rocks, which are separated from each other by an erosional unconformity marked by a conglomerate (Singh, 1988). The Raialo is dominated by marble, the Alwar by quartzites, and the Ajabgarh by calcareous schist.

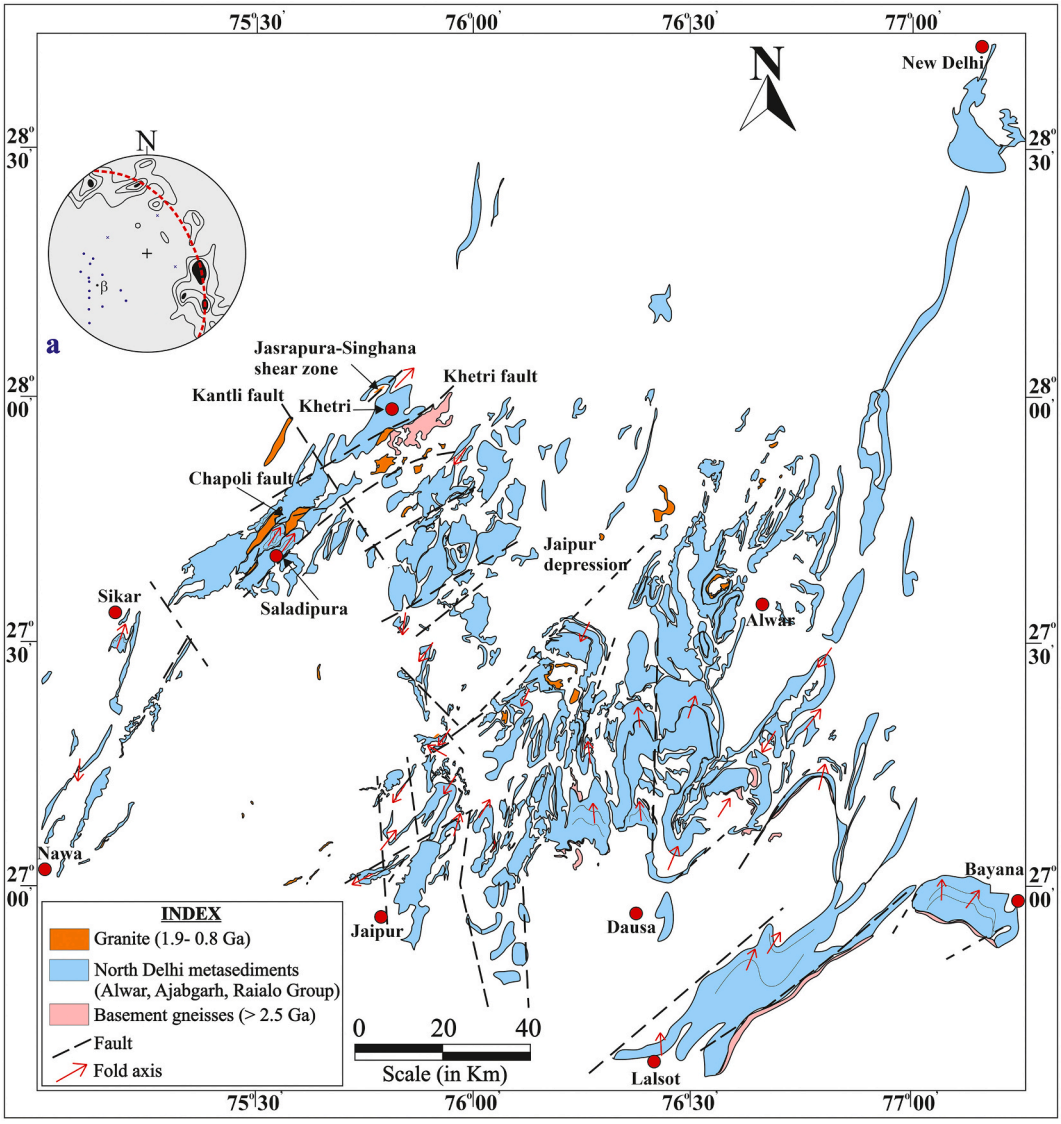

Fig. 5. Geological map of the North Delhi Terrane, drawn after Heron (1953) (a) Stereoplot shows NS1 plot, contours shows girdle distribution with β axis (NF2 fold axis) plunging towards the SW (Ray, 1974a).

Rift-related metavolcanic rocks occur as conformable bands within the metasedimentary sequence. The sediments were deposited in a continental rift setting within fault-bounded grabens that formed over the Archean basement rocks belonging to Bhilwara Terrane. The basement comprises gneisses and schists with ca. 2.5 Ga old granite intrusive (2529.60 ± 6 Ma, Jhiri granite Misra et al., 2020; Table 1) and is exposed near Lalsot and Bayana (Singh, 1988) and Khetri-Nawa (Gupta et al., 1998); in most places, these are covered by alluvium (as in the Dausa uplift). The metasediments of the terrane are syntectonically intruded by several granite plutons (Jasrapura, Paniaras, Seoli, Chapoli, Gothra- Gupta et al., 1998). Syn-SDT orogenic granites (< 0.87 Ga) also intruded at several places. Jasrapura granite representing Andean-type arc magmatism is the oldest intrusive yielding an age of 1821.7 ± 0.4 Ma (Kaur et al., 2009). The pluton occurs at the core of an NF2 antiform and bears the earliest solid-state fabric belonging to NF2 folding and thrusting, based on which it has been interpreted to be *syn*-NF2 (Gupta et al., 1998). However, the absence of any syn-NF2 magmatic fabric could put it in pre-NF2 age as well. Similarly, the Gothra granite showing pre- to syntectonic nature has an age of 1691 ± 4 Ma (Knight et al., 2002) and other plutons, some of which have been explained to be of extensional origin, show an emplacement age ranging from 1.7–1.5 Ga (Kaur et al., 2013, 2017). It suggests that the NDT sedimentation happened between 2.5 and 1.8 Ga and that the orogeny was initiated as early as ca 1.8 Ma (Table 2). Ductile deformation in the basement was synchronous with sedimentation in parts of the Khetri belt (Gupta et al., 1998). SEDEX-type Cu-deposits later hydrothermally remobilized along shear zones occur at Khetri (Roy Chowdhury and Das Gupta, 1965; Ray, 1974a; Sarkar and Dasgupta, 1980). Uranium mineralization in the albitite vein emplaced along the shear zone lies in the Khetri belt (Ray, 1987; Mishra et al., 2018) and unconformity-based U-mineralization is associated with the Lalsot-Bayana belt (Goyal et al., 2013). The grade of metamorphism of the terrane increases westward, from sub-greenschist facies in the Lalsot-Bayana belt (Mehdi et al., 2015) to amphibolite facies in the Alwar-Jaipur belt (550 °C/4 kbar, Sharma, 1988) and the Khetri-Nawa belt (600 °C/5 kbar, Lal and Shukla, 1975; Sarkar and Dasgupta, 1980). The Khetri-Nawa belt has produced a monazite age ranging from 1100 ± 20 Ma to 950 ± 16 Ma with several spot ages at 1506 Ma and 1627 Ma (Pant et al., 2008, Table 1). This indicates that the end stage of NDT orogeny extended up to 0.96 Ga. Thus North Delhi orogeny is constrained between 1.8 and 0.96 Ga (Table 2). This overlaps with Aravalli orogeny, which will be discussed in chapter 2.3.

2.2.2. Small scale structures

The rocks of the NDT are folded during an initial stage of coaxial folding between NF1 and NF2, along a NE-SW to N-S axis (Fig. 6a). Coaxial folding has produced a type 3 interference pattern of Ramsay (1967). The NF1 folds are tight to isoclinal (Fig. 6b) and are associated with NS1 axial planar schistosity, parasitic folding (Fig. 6c), and limb boudins. The NF2 folds are open and upright (Fig. 6a) and their formation changed the orientation of the NF1 folds to recumbent/reclined, inclined and upright due to coaxial folding. The NF3 folds are oriented in NW-SE to E-W direction (Fig. 6d) and their superposition has produced dome- and basin-structures with the NF2 folds.

2.2.3. Large scale structures

Small scale structures are repeated on the large scale too. The Khetri belt (around Saladipura) is deformed by three folding phases (Ray, 1974a), the NF1 and NF2 are coaxial along the NE-SW axis, produced by buckling due to NW-SE shortening. The stereoplot (Fig. 5a) describes the girdle distribution of the NF1 axial plane, the β-axis indicating the NF2 fold axis plunges to the SW. The NF3 fold has a NW-SE trending fold axis and is formed in response to NE-SW directed compression. NF1 and NF2 fold axes show plunge reversal and dome- and basin-structures due to the superimposition of NF3 on NF2. The NF3 fold axis shows plunge reversal due to variation in the attitude of the early folded surface. Further, the ductile shear zones are developed synkinematically with the NF2 folding (NF2 thrusts). The Jasrapura-Singhana thrust (Fig. 5) shows an eastern vergence (Gupta et al., 1998). Late-stage brittle faults cross-cut the NDT sequence e.g. Chapoli fault, Kantli fault, etc.

2.2.4. Lalsot–Bayana belt

The Lalsot-Bayana belt is marked by a similar structure as the Khetri belt; the belt shows overprinting of NE-SW coaxial folding on the basement rocks. The erosional unconformity and the overlying formations describe N-S to NE-SW trending large-scale NF2 folds (Goyal et al., 2013). Similar folds along a N-S to NNE-SSW axis are observed in North Delhi rocks of the Jaipur-Alwar belt. The N-S and NE-SW faults transect the basin offsetting the fold limbs and axial plane (Das, 1988).

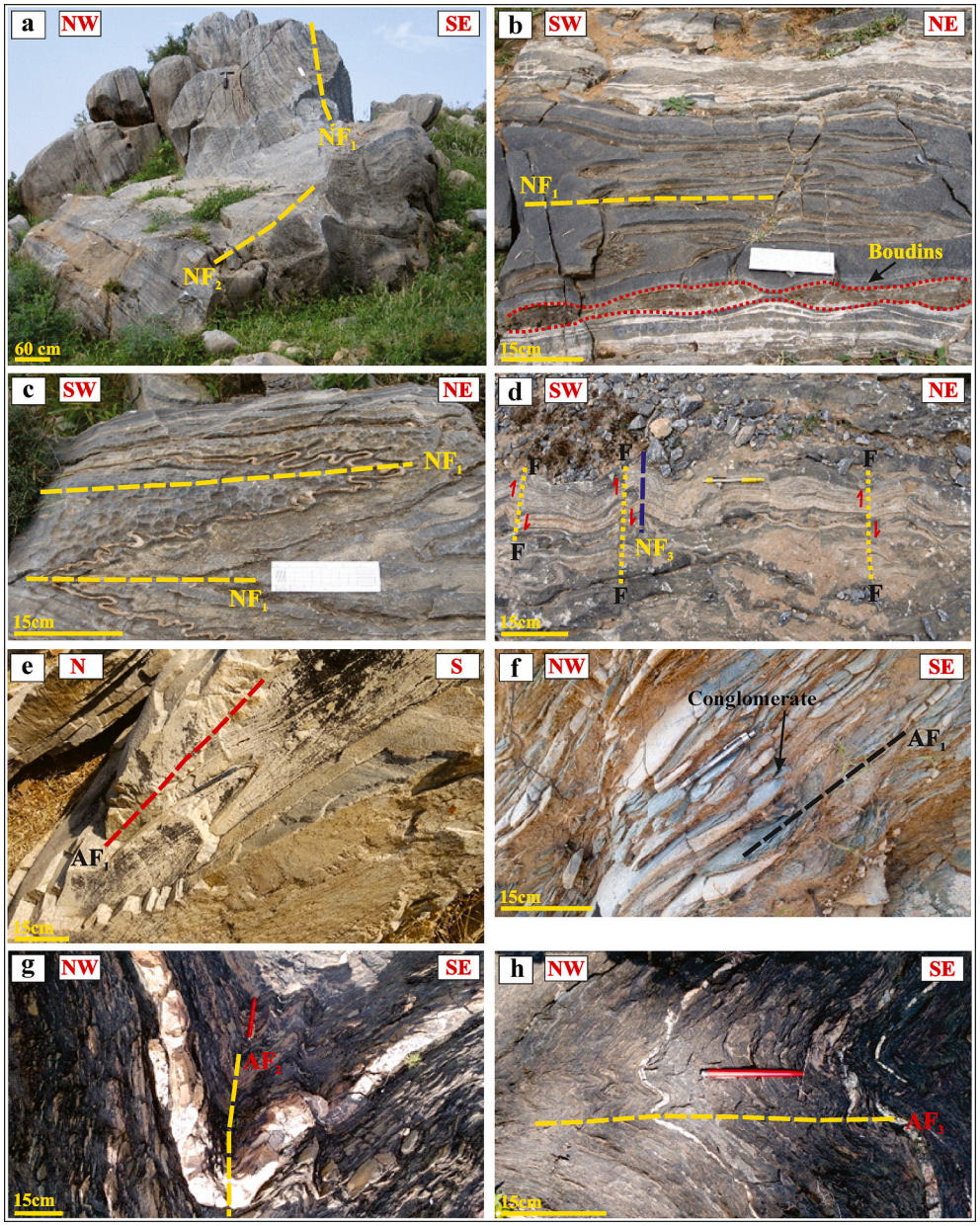

Fig. 6. (a) Coaxial folding between the NF1 and NF2 folding phases, horizontal section, looking towards the NE, (b) NF1 isoclinal fold with limb boudins, horizontal section, looking towards the NW, (c) Parasitic folds associated with NF1 folds, horizontal section, looking towards the NW, (d) NF3 folds with normal slip faults, horizontal section, looking towards the NW, (e) AF1 fold, horizontal section, looking towards the E, (f) Stretched conglomerate parallel to the AF1 axis, vertical section, looking towards the NE, (g) AF2 fold, vertical section, looking towards the NE, (h) AF3 fold. Horizontal section looking towards the NE (Photo courtesy: North Delhi photographs are by Dr. Harish Ahuja and Aravalli Photographs are by Prof. N K. Chauhan).

2.3. Aravalli Terrane

2.3.1. Geological settings

The Paleoproterozoic Aravalli Terrane extends from the north of Kankroli to Champaner in the south (Fig. 1b; Gupta et al., 1980). We are excluding the volcano-sedimentary belts exposed at Hindoli, Jahazpur, Pur-Banera, and Rajpura-Dariba from the Aravalli Terrane and included them in the Bhilwara Terrane, as they have debatable ages (Archean to Paleoproterozoic, discussed chapter 2.4). The Aravalli Terrane has an N-S trend with a triangular geometry, with a narrow width in the north and a wider width in the south (Fig. 1b, Fig. 7). The terrane shares a wavy and E-W trending contact to the north with Archean basement rocks of Sandmata Complex (BGC 2) (Fig. 1b). The terrane can broadly be divided into two parts by the Rakhabdev shear zone, the eastern (shallow water facies) and western parts (deep water facies) (Fig. 7). The Rakhabdev shear zone is considered to be a belt of ophiolites and represents a suture in the subduction zone of the Aravalli Terrane (Gupta et al., 1997). Though Purohit et al. (2015) considered the continental setting for the ultrabasic rocks, the antigorite-serpentinite in the rocks suggests its derivation from a mantle wedge in an exhumed subduction zone (Sarkar et al., 2020). The eastern part of the Aravalli Terrane is dominated by mica schist, metavolcanics, marbles, dolomite, conglomerate-paleosol (De Wall et al., 2012) and quartzite. The sequence rests unconformably over the ca. 3.2 to 2.6 Ga basement granite and gneisses belonging to BGC-1 (Referred to as Mewar Craton) (Untala granite, Mewar gneiss, Rakhiawal gneiss, MacDougall et al., 1983; Wiedenbeck and Goswami, 1994; Roy et al., 2001; Table 1). Further, these are intruded by 2026 ± 54 Ma old Ahar river granite (Wiedenbeck and Goswami, 1994) and 1870 ± 200 Ma old Amet granite, these are *syn-* sedimentary intrusives in the Aravalli basin (Choudhary et al., 1984). The basement gneisses are folded with cover metasediments and presently occur as inliers at Sarada and Kankroli. Contrastingly, the western part of the Aravalli Terrane is micaceous with interlayers of quartzite. There is an exposure of basement rock at Bagdunda. The eastern part of the terrane shows an increase in the grade of metamorphism from south to north, the Banas shear zone probably marks the dividing line between low-grade and high-grade rocks (Banas dislocation zone, Sinha-Roy et al., 1993). The Aravalli rocks in the north of Banas shear zone, exposed around Kankroli and Nathdwara, show amphibolite to upper amphibolite facies of metamorphism at 1784 ± 92 Ga (Chander et al., 2021) and migmatised syn-AF1 and grades into the migmatites of the Sandmata/Mangalwar Complex (Naha and Halyburton, 1974). Further, granulite and charnockite were tectonically emplaced/exhumed through thrusting along AF2 thrusts, into Sandmata Complex, which was considered to have resulted from arc magmatism and later metamorphosed in granulite facies over a period of 1.7 to 1.6

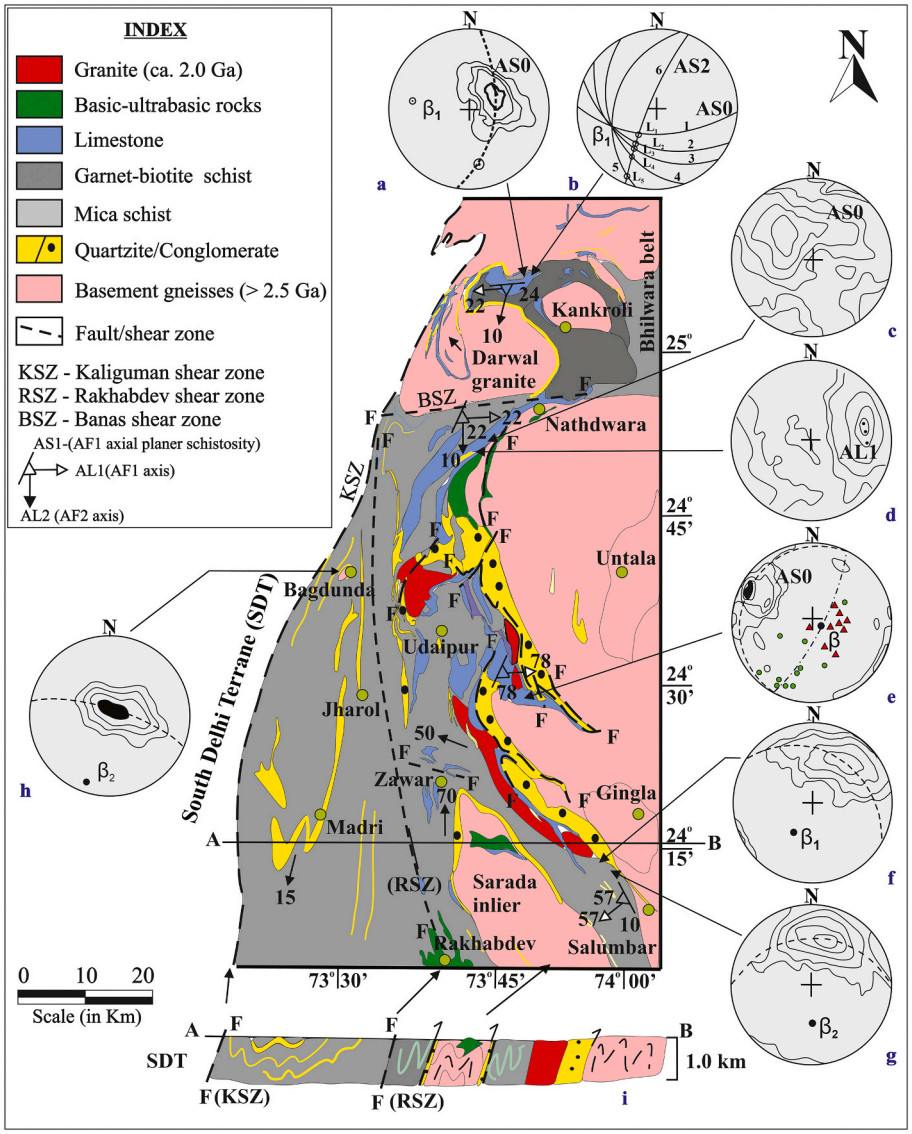

Fig. 7. Geological Map of the Aravalli Terrane (drawn from Heron, 1953) (a) Stereoplot, contours show the distribution pattern of bedding plane AS0. The β- axis indicates westerly plunge of the AF1 fold (Naha and Chaudhuri, 1968), (b) Stereoplot showing bedding planes folded by AF1 fold, axis shows an SW plunge. AF2 fold axial plane is oriented NE-SW (AS2) (Naha and Chaudhuri, 1968). AF2 fold axis shows a variable trend as the AF2 fold is developed on variably oriented AS0 surface, (c) Stereoplot showing contours of AS0 pole plots from west of Nathdwara, the maximum lies in the NW quadrant suggesting NE-SW strike of the AS0 planes (Naha and Halyburton, 1977), (d) Stereoplots showing contours of AL1 plots from west of Nathdwara, the maximum lies in ENE direction, suggesting plunge of AF1 fold axis (Naha and Halyburton, 1977), (e) Stereoplots showing contours of AS0 plots from southeast of Udaipur, a well-defined girdle with the maximum lies in WNW direction, suggesting a plunge of the AF1 fold axis towards ESE (Roy and Nagori, 1990), (f) Stereoplot showing AS0 planes, the fold axis AF1 is in SW direction, Salumbar area (Naha and Mohanty, 1988), (g) Stereoplot showing AF2 fold axis in southern direction, Salumbar area (Naha and Mohanty, 1988), (h) Stereoplot showing AF2 fold axis in southern direction, Bagdunda area (Sharma et al., 1988), (i) Cross- section across the Aravalli Terrane showing different faults and formations. There is a mylonitic zone marked by thrust kinematics between the rock cover and basement.

Ga (Sarkar et al., 1989; Roy et al., 2012). The nepheline syenite was emplaced at Kishangarh at 1.4 Ga (Kaur et al., 2021). The AF1-AF2 folding probably occurred somewhere during 1.7 to 1.4 Ga. Thus, the Aravalli orogeny is considered to have initiated at 1.7 Ga presumably coeval with North Delhi orogeny (1.8 Ga). Aravalli sediments are 2.5 Ga to 1.7 Ga old. Extensive migmatisation has obliterated the basement-cover relationship. Heron (1953) mapped the higher-grade rocks north of the Banas shear zone as the Raialo series of the Eparchean age (Fig. 1a) while Gupta et al. (1980) included them in Paleoproterozoic Aravalli Supergroup (Fig. 1b).

The Aravalli Terrane in the south near Champaner is intruded by the 965 ± 40 Ma old late-tectonic Godhra granite (Gopalan et al., 1979). With reference to the ages for the major dynamothermal events, anataxis of the metasediments and emplacement of granulites in the Sandmata Complex, the Aravalli orogeny is constrained between 1.7 and 0.96 Ga (Table 2) and is considered to be part of the globally occurring Nuna orogeny that gave rise to Columbia Supercontinent. But the ca. 965 Ma overprint suggests that the Grenvillian orogeny, that produced Rodinia Supercontinent, affected the previous orogen. Comparing it with the events in SDT, the rifting and sedimentation in SDT was coeval with the later part of the Aravalli orogeny (Table 2).

2.3.2. Small- and large-scale structures

The eastern part of the Aravalli Terrane has been folded into recumbent/reclined, isoclinal folds during a first folding phase (AF1) with an *E*-W oriented fold axis (Fig. 6e). The rocks are marked by a pervasive AF1 axial planar schistosity (AS1). In Nathdwara and Kankroli areas, the Aravalli mica-schist is migmatised and migmatisation bands are parallel to a first schistosity phase (AS1), indicating the syntectonic nature of migmatisation with AF1 folding. The basement rocks are also imprinted by AS1 schistosity and have been migmatised. The conglomerates are extremely stretched parallel to the AF1 axis and lithological competent layers formed boudin structures (Fig. 6f). The AF2 folds are open to tight and upright (Fig. 6g) indicating vertical flow during AF2 folding. The superposition of AF2 on AF1 has resulted in the folding of the axial plane and the axis of the AF1 folds and produced a mirror-image pattern. AS2 is represented by crenulation and pressure solution cleavage. Two sets of lineation (AL1 and AL2) each belonging to AF1 and AF2 folds are present on the schistosity plane. AF2 thrusts were present parallel to the axial plane of the fold. The AF3 folds are a set of open folds with crenulation cleavage and axial parallel shears (Fig. 6h) in the NW-SE direction with the vertical flow that is superimposed on AF2 folds to produce dome- and basin- structure.

The large-scale structure also reflects a similar folding pattern. Stereoplots Fig. 7a shows the N-S trend of the AS0 and the fold axis AL1 (β_1) is oriented towards the W confirming the reclined nature of the AF1 fold. The AF1 folds are refolded by AF2 folds along the N-S axial plane (AS2) and axis (AL2) (Fig. 7b). The hook syncline, hammer-head syncline, and main Raialo syncline are the large-scale dome- and- basin structures in this area produced from the superimposition of AF3 on AF2. The area to the west of Nathdwara (Fig. 7) shows NE-SW bands of marble, mica schist, and metavolcanic overlying the basement. The rocks including the basement and metasedimentary covers record the reclined AF1 folds with NE-SW axial plane (AS0) (Fig. 7c), and ENE plunging AF1 axis (AL1) (Fig. 7d). The area SE of Udaipur where metasediments are interlayered with ca. 2.0 Ga (Ahar River granite, Wiedenbeck and Goswami, 1994) granites are folded by AF1 reclined folds (Roy and Nagori, 1990). Several basin margin faults reactivated as AF2 thrust-strike slip shear zones are present and some of them are also folded. The contours in Fig. 7e indicate the distribution of poles of AS0 that shows an average dip towards the SE and the pole of the girdle shows the AF1 (β-axis) in the SE. The Salumbar area displays southwesterly dipping beds as the result of multiple-stage folding (Naha and Mohanty, 1988). The AF1 is reclined with SW plunge (Fig. 7f) and the AF2 folds are at a high angle to AF1 and oriented in the N-S direction (Fig. 7g). Away from the basement, at Zawar Mala, the AF1 folds are reclined/recumbent, but the fold axis is plunging in N-S to NE-SW direction. As a result, the interference pattern between AF1 and AF2 has been coaxial, and hook-shaped folds are produced in the rocks. Extensional crenulation cleavage and thrusts are associated with the AF2 fold (Roy, 1995; Biswal et al., 1997). The eastern margin of the Zawar Mala hill is marked by AF2 thrusts with strike-slip reactivation (Roy, 1995). The AF3 folds are usually upright with an NW-SE axial plane and the flow direction is vertical. As a result, the interference between AF2 and AF3 produced dome- and basin- structures in most instances. However, at Mochia Mogra Hill, north of Zawar Mala, the AF3 folds show horizontal flow resulting in the folding of the axial plane and axis of AF2 folds producing a mirror-image pattern. This folding occurred under NW-SE oriented AF3 strike-slip fault activity which was responsible for horizontal flow during AF3 folding. The Banas shear zone shows a nearly E-W trend and dextral strike-slip kinematics (Sinha-Roy et al., 1993). The lithological units across the shear zone have been aligned parallel to the strike of the shear zone. The rake of the stretching lineation increases towards the west, suggesting more thrust-slip components. The shear zone has been reactivated later as brittle faults and cross-cut the SDT, Mangalwar Complex, and the Great Boundary Fault.

The western part of the Aravalli Terrane is free from basement rocks except at Bagdunda where a domal outcrop of basement gneisses is exposed (Sharma et al., 1988). At Bagdunda dome including some of the areas further north, close to the south of Kankroli, the AF1 fold axes have an E-W orientation like the eastern part of the Aravalli Terrane (Hahn et al., 2020) and this is superimposed by N-S trending AF2 folds (Fig. 7h). In other parts, where thin layers of quartzite are interbedded within mica-schist (e.g. Madri, Fig. 7), the AF1 folds developed along the N*E*-SW axis and have been coaxially refolded by upright AF2 folds.

A cross-section (Fig. 7i) across Aravalli Terrane passing through the basement gneisses exposed in Sarada inlier (Heron, 1953; Gupta et al., 1997) shows westerly dipping formations. The basement rock in the inlier is flanked by a conglomerate, which is folded by AF2 fold. Both the margins of the inlier show westerly inclined AF2 thrusts (~ 65 degrees) with well-developed quartzofeldspathic mylonites. The conglomerate and the Aravalli rocks are mutually thrusted over the basement rocks.

2.3.3. Southern Aravalli

The Aravalli Terrane to the south of Rakhabdev is characterized by mica schist with a higher number of quartzite bands (Fig. 8). The areas around Lunavada and Champaner are rich in such quartzite bands, which have undergone large-scale folding with varying wavelength and amplitude (Mamtani et al., 2002; Mamtani and Greiling, 2005; Joshi, 2019; Joshi and Limaye, 2020). In the Lunavada area, the coaxial folding between AF1 and AF2 produced a type 3 interference pattern that is preserved. The AF1 folds are recumbent/reclined with a N*E*-SW oriented fold axis and the AF2 folds are upright with a NE-SW oriented axial plane. AF3 folds are prominently developed along the NW-SE fold axis and produced dome- and basin- structures with AF2. At several places, the flow direction of AF3 folds has been horizontal and this rotated the axial plane and axis of the AF2 folds producing a type 2 or mirror-image pattern. Due to this pattern, the AF2 folds have assumed an E-W trend on the E-W limb of the AF3 fold. This trend continues to the Champaner areas where the large-scale AF2 folds have an E-W oriented fold axis and plunge to the west. The Godhra granite (ca. 960 Ma, Gopalan et al., 1979) has intruded syntectonically with AF3 folding, suggesting the age of AF3 folding to be ca. 960 Ma. The granite has magmatic foliations striking parallel to the AF3 fold axial plane. NW-SE lineaments are prominent in granite. Another set of folds (AF4) with a N*E*-SW trending fold axis is developed on the E-W limb of the AF3 fold, which has produced domes with AF2 folds to the east of Champaner.

2.4. Bhilwara Terrane

2.4.1. Geological settings

The Archean Bhilwara Terrane comprises the basement rocks of the

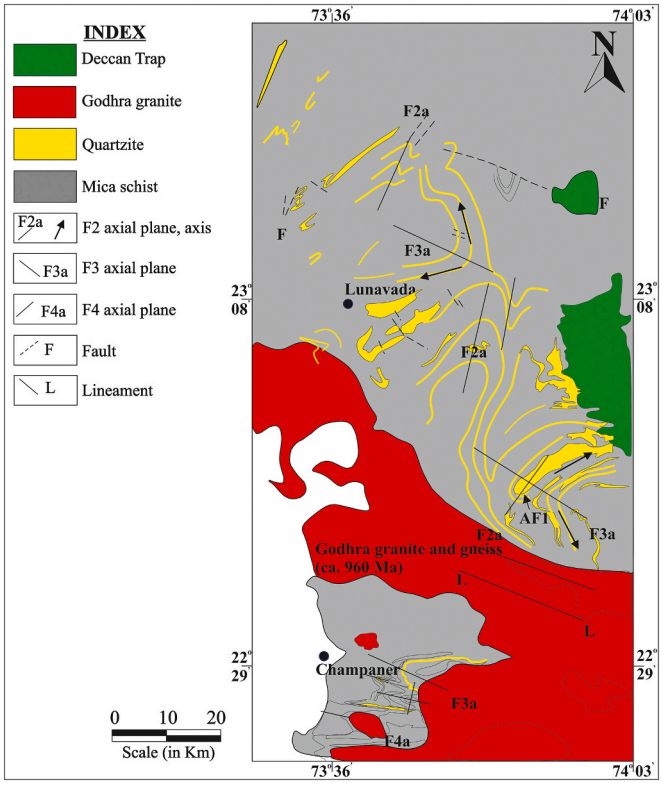

Fig. 8. Geological map of the Lunavada and Champaner area, Aravalli Terrane (drawn from Gupta et al., 1980).

ADMB, which is also referred to as the Banded Gneissic Complex i.e. BGC-1 and BGC-2 (Heron, 1953; Ahmad and Mondal, 2016), though both are not the same. The Bhilwara Terrane comprises the Sandmata and Mangalwar complexes. Both are characterized by migmatites with interlayers of amphibolite and pelitic schist restite bands. The Mangalwar Complex is intruded by the 2610 ± 50 Ma old Berach granite (Sivaraman and Odom, 1982), The Jahazpur granite (2538 ± 5 Ma, Dey et al., 2019) and the Malola granite (2538 ± 11 Ma, D'Souza et al., 2019, 2020) (Table 1). The Sandmata Complex is intruded by the Dharwal granite (2905 ± 0.3 Ma, Roy et al., 2012) and the Nagar granite (Near Bhinai, 2548 ± 6 Ma, Kaur et al., 2021). Similar granite intrusions are observed in the basement rocks of the NDT. Thus, the Bhilwara orogeny, which is constrained at 2.6 Ga stabilized the NW India shield by the intrusion of these granites (Table 2). However, the basement is tectonothermally rejuvenated by The Aravalli and Delhi orogenies. The 1725–1622 Ma old granulites and charnockites were thrusted within the Sandmata Complex during the Aravalli orogeny (Sarkar et al., 1989; Fareeduddin, 1998; Roy et al., 2012), The Kishangarh nepheline syenite intruded at 1490 ± 150 Ma (Crawford, 1970), and the SDT-granites intruded at 0.88 Ga. Further, the Aravalli and Delhi orogenic events have deformed the Sandmata rocks along the terrane margin (Naha and Halyburton, 1974; Sen, 1980; Srivastava, 2001; Roy et al., 2012, 2016). Thus, the older ages of the Mangalwar and Sandmata complexes are reset to younger ages, particularly in the northern part of the Banas shear zone (Bhowmik and Dasgupta, 2012; Ahmad and Mondal, 2016; Kumar et al., 2019; D'Souza et al., 2021).

The Mangalwar Complex contains several narrow linear volcano-sedimentary belts (e.g. conglomerate-carbonates-BIF-quartzite-garnet-biotite schist-amphibolite sequence) with sulfide deposits, e.g. Rajpura-Dariba, Pur-Banera, Jahazpur-Hindoli, Rampura-Agucha, and Sawar (Fig. 9). The belts owe their origin to rifting of the basement and have subsequently undergone compressional tectonics with extreme flattening, thrusting, and dextral shearing along with the basement (Sinha-Roy et al., 1998), which led to the obliteration of any unequivocal evidence of the basement-cover relation. Individually they appear as thrust belts within the migmatitic country rock. Further, the galena samples analysed from Dariba mines produced U—Pb zircon age 1808–1931 Ma (Deb et al., 1989), and zircons from a sample of massive rhyodacite in the Hindoli group yielded a concordia age of 1854 ± 7 Ma (Deb et al., 2002). Based on these ages the belts are considered equivalent to the Proterozoic Aravalli Terrane (Roy and Jakhar, 2002; D'Souza et al., 2019; Chander et al., 2021). But none of these previous studies, is the work of Raja Rao et al. (1971) rebutted, who finds that the Berach granite is intruded in the Hindoli group. Further, chemogenic iron ore deposits of these belts resemble that of Archean iron ore (Sharma et al., 2020), the Hindoli group chemically shows a similarity in REE pattern to that of BGC (Saxena and Pandit, 2012), Rajpura- Dariba belt carries komatiite rocks of Archean affinity (Yadav, 2015). In addition, ca. 3.2 Ga old greenstone belts are associated with the Mangalwar complex (Roy et al., 2001). All this evidence cast uncertainty about the age of these volcano-sedimentary belts. We therefore interpret that part of the volcano-sedimentary sequence could be Neoarchean and part to be Paleoproterozoic as explained by Sinha-Roy and Malhotra (1989) for Hindoli (Archean) and Jahazpur (Proterozoic) groups. Hence, these are time transgressive sequences straddling the Eparchean interval.

The ADMB has a prominent syntaxial bend in the eastern part at the Udaipur-Chittorgarh axis affecting the Mangalwar Complex, the volcano-sedimentary belts, the Delwara lineament and the Aravalli-Sandmata belts. The Banas shear zone occurs over the syntaxial bend (Fig. 1b). The belts located to the south of this axis are NW-SE trending and have preserved the oldest rock in the ADMB (Mewar gneiss, 3281 ± 3 Ma, Wiedenbeck and Goswami, 1994; Untala granite, 3500 Ma, MacDougall et al., 1983, Table 1). Belts to the north of the axis show N-S and N*E*-SW trends. The maximum age of these rocks in the north is ca. 2.9 Ga (Darwal area, Roy et al., 2012). The curvature of the syntaxial bend gradually reduces from east to west, the maximum curvature occurs on the Mangalwar Complex, and only has a minor impact on the Aravalli-Sandmata belts, and the SDT remains straight while greatly pressed in the centre and flared on either end. The bend was produced by indentation tectonics of the Berach granite and its precursor during a collision between Bundelkhand Craton and Marwar Craton. Since the SDT is affected by this indentation tectonics, it is interpreted that the indentation tectonics was synchronous with the South Delhi orogeny. The Berach granite acted as the indenter as the Mangalwar, as well as Aravalli-Sandmata belts, were arched around it. The role of Berach granite as an indenter during Bhilwara and Aravalli orogenies is difficult to interpret with the current data set.

2.4.2. *Small- and large-scale structures*

The migmatites exhibit complex flow folding depicting multiple generations of folds and shear zones. The volcano-sedimentary belts within the migmatitic country rock of the Mangalwar Complex preserve at least three stages of folding (BF1-BF3). The BF1 folds, which are oriented in the *E*-W direction, in these belts are isoclinal and reclined. These are associated with BS1 schistosity/gneissosity. BF1 is refolded by NE-SW trending BF2 fold, which is extremely flattened and overturned to the NW or SE. The superimposition of BF2 on BF1 has produced a mirror-image pattern similar to the eastern part of the Aravalli Terrane. Crenulation and compositional boudins are associated with the BF2 folds. The BF2 axial planar shears are very prominent which are marked by thrust kinematics overprinted by dextral strike-slip kinematics (Sinha-Roy et al., 1998). The BF3 folds are along an NW-SE to E-W trend and produced plunge reversal in BF1 and BF2 folds. Large-scale structures of these belts are a replica of small-scale structures. The Sawar synform (BF2) has been inverted to an antiform in the southern end (Fig. 9, Ray, 1974b). The northwesterly inclined Jahazpur thrusts demarcate the belt from the basement and Hindoli Group (Sinha-Roy and Malhotra, 1989). The Jahazpur Group exhibits a NE-SW trending BF2 synformal structure, which is extremely flattened and overturned to the SE. It has undergone an initial BF1 folding with an E-W to NW-SE

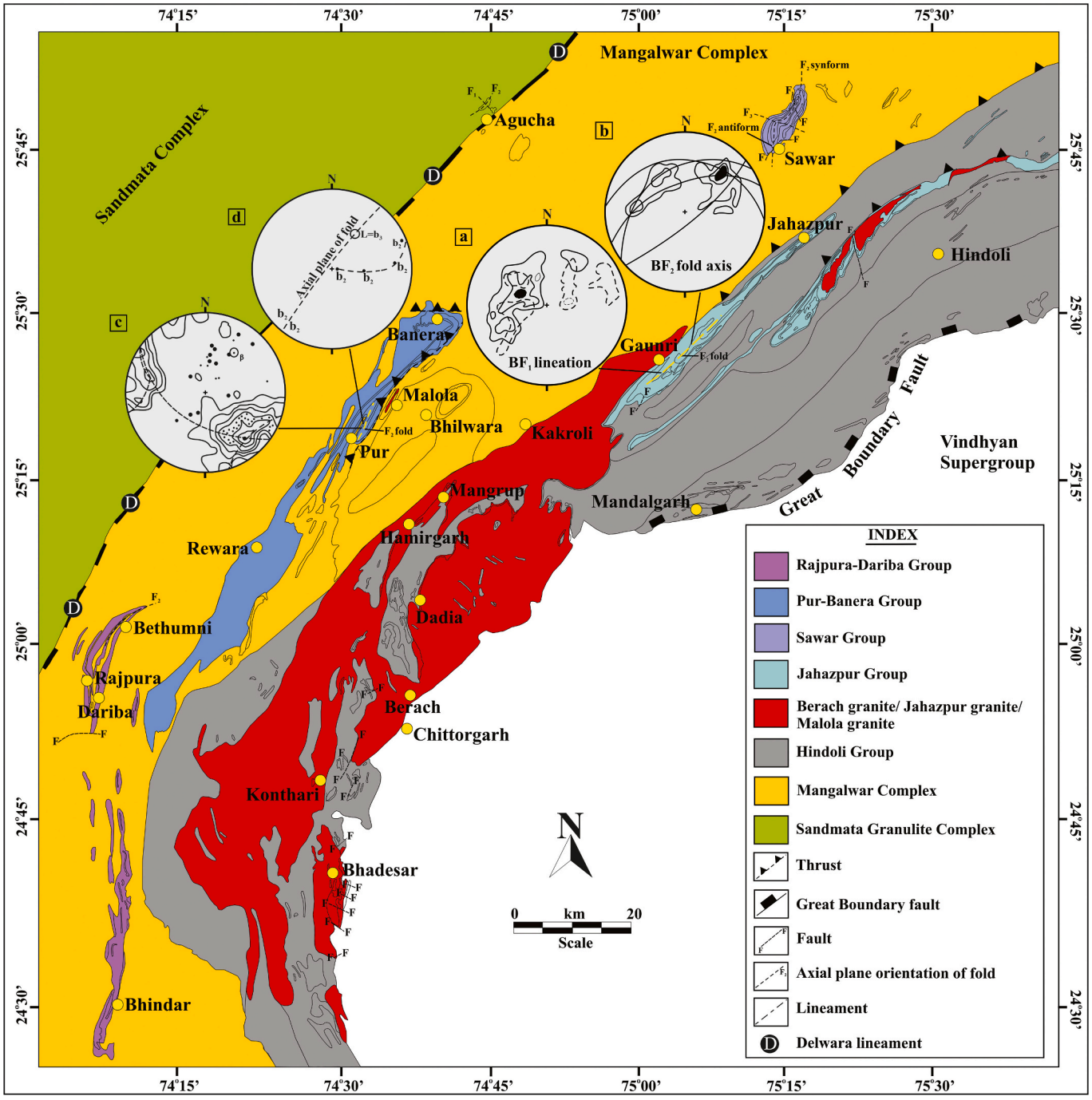

Fig. 9. Geological map of the volcano-sedimentary belts within the Mangalwar Complex. Stereoplots 9a, 9b (Sinha-Roy and Malhotra, 1989) belong to the Jahazpur belt while 9c, 9d (Dasgupta, 1982) belongs to the Pur-Banera belt (For stereographic data interpretation refer to the text).

trending fold axis which is superimposed by NE-SW BF2 folding. As a result, the early fold axes show varied orientations (Fig. 9a) while the BF2 fold axes point to the NE (Fig. 9b). The Jahazpur belt unconformably overlies Hindoli Group and the later shows one phase of folding before the onset of the BF1 folding event in both Hindoli as well as the Jahazpur belts. The Great Boundary Fault demarcates the Hindoli Group from the Vindhyans. It is a ductile shear zone that has been reactivated as a normal fault multiple times (Sahay and Srivastava, 2005). The Pur-Banera belt represents an extremely compressed BF2 fold with axes oriented in NE-SW direction (Fig. 9c, Dasgupta, 1982; Chowdhury and Bosevska, 2017; D'Souza et al., 2021). The early fold axes rotate in small circle suggesting the effect of superposed folding produced from buckling (Fig. 9d). Thrusts having NE-SW and E-W strikes occur in the eastern and northern margin of the belt respectively (Fig. 9) (Kumar et al., 2019). The Rajpura-Dariba-Bethumni belt has a crescent geometry due to the effect of the syntaxial bend. The BF2 thrusts are prominent inside the belt (Yadav, 2015). The Rampura-Agucha belt shows multiple phases of folding with N-S doubly plunging BF2 folds (Bhatnagar and Mathur, 1989) with a prominent central thrust that runs most likely parallel to the Delwara lineament (Gandhi et al., 1984). The granulite pockets within the Sandmata Complex and Kishangarh nepheline syenite were exhumed and emplaced along NE-SW trending BF2 thrusts. The granulites as well as adjoining migmatised rocks were mylonitised and folded by multiple-generation of folds (four stages of folding, Guha

and Bhattacharya, 1995; Roy et al., 2012, 2016). The BF3 folds probably belong to a deformation phase around ca. 950 Ga. The folds have been converted to sheath geometry due to higher strain in the shear zone. Further, thrusting along Kaliguman thrust has produced sheath folds in the basement (Srivastava, 2001).

3. Discussion

3.1. Geometry of the orogen

The geometry of an orogen is largely controlled by its deformation structures such as large-scale folds, shear zones, and faults. The Bhilwara-, Aravalli-, North Delhi-, and South Delhi terranes form a set of parallel terranes accreted to the ADMB during different orogenic episodes. Each of these terranes has undergone compressional tectonics marked by superimposed folding and shearing. The folds show varied orientations depending on their mutual relationship and flow direction and have left an impression on the geometry of the orogen. Leaving aside the eastern part of the Aravalli Terrane and Mangalwar Complex to the south of the Udaipur-Chittorgarh syntaxial axis, the individual terranes in the Aravalli orogen display a N*E*-SW trend that is largely attributed to the second fold in each of the terrane (DF2, NF2, AF2, and BF2 respectively), which occurs as meso- to large- scale upright folds and have developed in different period (Table 2). The NW-SE trend of the lithological units in the southern part of the Mangalwar Complex is ascribed to the syntaxial bend. Further, the second folding event in each terrane is associated with axial planar thrusts that are sub-vertical to steeply dipping. Excess shortening has progressively led to strike-slip shearing along such a thrust plane. These thrusts with superimposition of strike-slip kinematics have provided extreme linearity to the lithological units e.g. the western part of the ADMB (Bar-Babra-Ajmer area, Fig. 1b) contains several linear ridges that reflect the presence of DF2 thrusts like the PSZ, KSZ, and thrusts bounding the Beawar and Anasagar gneisses. The Jahazpur, Rajpura-Dariba, and Pur-Banera belts have acquired extreme linearity due to the tightness of the BF2 fold and the presence of BF2 thrusts. Contrarily, the outcrops of the North Delhi Terrane are well spread out due to the openness of the NF2 folds (Fig. 5). The third folding event that has affected different terranes at different periods (Table 2), has manifested as open folds, sometimes as conjugate kinks and warps (DF3, NF3, AF3, and BF3). As the fold is developed in polyclinal fashion, the axial plane of the fold shows orientations in *E*-W, NW-SE, and NE-SW directions with the vertical flow. The superimposition of the third generation of fold on the second generation fold has created a dome- and basin- structure. In this interference pattern, the axial plane of the earlier fold remains planar and the axis is curved. Therefore, large-scale domal outcrops are present at the Sarada inlier, the Bagdunda dome, the Babra-Beawar transect, etc. However, in certain areas at Zawar, Ambaji, Lunavada, and Champaner (Figs. 4, 7, 8), the third folding phase is associated with axial planar strike-slip shear zones. As a result, the flow direction is modified to *E*-W in the horizontal plane. The superposition of such folds on folds of the second folding phase has resulted in the folding of the axial plane and axis of the second fold to the E-W direction creating mirror-image interference patterns. The Lunavada and Champaner areas in Aravalli Terrane exhibit the E-W trend of the lithological units. The Godhra granite interrupts the continuity of the Aravalli metasediments to the Champaner area, however, tracing the quartzite bands from Lunavada to Champaner and analyzing the structures in Godhra granite demonstrates that the Champaner rocks are very much part of Aravalli Terrane and its present E-W trend is primarily due to AF3 folding.

The syntaxial bend on the eastern part of the ADMB is produced by the indentation tectonics of the Berach granite in the collisional front between the Bundelkhand Craton and Mewar Craton against the Marwar Craton. The Mangalwar, Aravalli and Sandmata belts are arched around the granite pluton while the SDT has been compressed to a narrow width between Todgarh and Kumbhalgarh due to strain concentration near the hinge of the arch. The fan-shaped geometry on the NE and SW ends of the SDT resulted from lateral extrusion of material. Several strike-slip faults (the conjugate pattern indicating NW-SE compression) occur in that narrow zone, and are oriented obliquely compared to the SDT producing an en échelon arrangement of the ridges. The Banas shear zone and its extended part run through the Mangalwar Complex in the east and SDT in the west (Fig. 1b, Fig. 7). The shear zone shows ductile as well brittle deformation suggesting its reactivation several times in different levels of the crust. The exposure of high-grade rocks including the Sandmata-Mangalwar complexes and migmatised belts of Kankroli and Nathdwara areas to the north of the Banas shear zone may be due to the south verging thrust kinematics of the shear zone, or tilting of the Aravalli Terrane towards the south. This has resulted in the uplift of northern blocks and exposure of deeper-level rocks through erosion. Further, the Aravalli Terrane shares an E-W margin with the Sandmata Complex. The structural-metamorphic fabric is orthogonal to the above margin. The high angle relationship could be attributed to such tilting of the block. Another important structure in the ADMB is the Sambhar-Lalsot geomorphologic gap which has created a discontinuity of the NDT into the Sandmata and Mangalwar Complexes. The creation of such a gap is attributed to the tilting of the Aravalli and Bhilwara Terrane to the south as well as to the presence of several shear zones as mentioned earlier.

3.2. Tectonic setting

The different compressional, extensional, and strike-slip (Fossen, 2010) tectonic deformation that affected the region have had major implications on the structural geology of the terrane. The SDT, NDT, and Aravalli terranes and the linear belts within the Mangalwar Complex were principally extensional basins formed by rifting of the granitic basement. These are marked by horst and graben structures, passive margins with synsedimentary bimodal volcanic and volcanogenic sulfide deposits (Biswal et al., 1998a; Deb, 2000; Singh et al., 2021). An NW-SE-directed extensional setting probably created such basins.

The terranes have undergone compressional tectonics that manifest through multiple generations of folding and ductile shearing. The folds are characterized by disharmonic folding, homogeneous flattening, axial plane cleavage refraction, and boudinaged folds (Fig. 3 and Fig. 6), which are characteristics of buckling and are attributed to compressional stress over horizontal to sub-horizontal beds (Fig. 10a). Coaxial folding between the first two folds along a NE-SW axis is observed in several parts of the terranes. The first fold is recumbent/reclined (Fig. 10b) and the second fold is upright and the axial plane is in a NE-SW direction, thus producing a type 3 interference pattern (Fig. 10d). This leads to the interpretation that an NW-SE directional shortening played an important role during each orogenic episode. The first fold was produced due to a simple shear strain where the intermediate strain axis was horizontal and aligned in the NE-SW direction (Fig. 10b). The recumbent attitude of the fold further indicates a sub-horizontal flow of the material. The most penetrative fabric (S1) in all the terranes is axial planar to the first fold, suggesting that a major tectonothermal event has taken place during that period. Subsequent folding is manifested as crenulations developed over the S1 fabric. One exception is the eastern part of the Aravalli Terrane and volcano-sedimentary belts of the Bhilwara Terrane that show the E-W oriented AF1 fold axis (Fig. 10c) and the second fold is in the NE-SW direction. As a result, type 2 interference patterns developed (Fig. 10e). In those areas, the metasediments and the granitic basement were together involved in folding. The rheological contrast between the basement and rock cover led to decoupling and larger strain concentration at the interface and, as a consequence, the AF1 fold axis was rotated progressively towards the transport direction (i.e. Fig. 10c, NW-SE to E-W, e.g. Ramsay and Lisle, 2000). The upright nature of the second fold indicates that a pure shear strain tectonic regime is responsible for its formation (Fig. 10d, e). The transition from simple shear to pure shear occurred when the metasediments along with

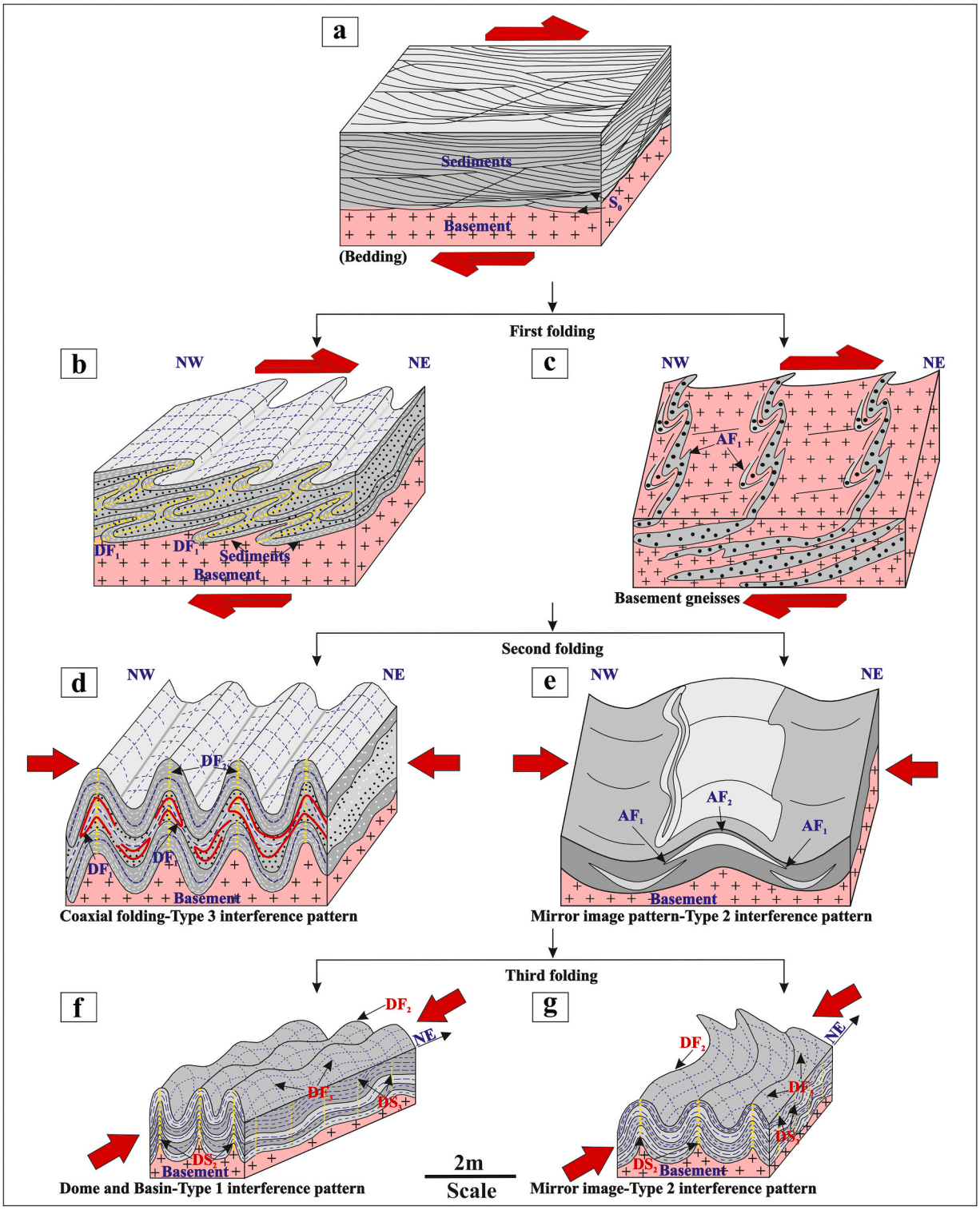

Fig. 10. Structural model showing generation of different phases of folding in the ADMB (a) Sedimentary beds showing gentle attitude, (b) First folding phase (DF1, NF1, AF1, and BF1) results from coupled shear, forming reclined and recumbent folds along a NE-SW axis, (c) High strain concentration in the interface between the basement and rock cover, as the basement and sediments were folded, the NE-SW first fold was reoriented to E-W direction. This can be observed in the eastern part of the Aravalli Terrane, Mangalwar Complex, and part of the South Delhi Terrane, (d) Second folding phase (DF2, NF2, AF2, and BF2) took place under NW-SE compression This coaxially refolded the first fold, producing Type 3 interference patterns, (e) Type 2 or mirror- image pattern developed due to the superimposition of second folds on E-W trending first folds. This is most common in the eastern parts of the Aravalli Terrane and the narrow linear belts in the Mangalwar Complex, (f) Type 1 interference pattern or dome- and basin- structure formed in response to the interference between NE-SW second folds and NW-SE trending third folds (DF3, NF3, AF3, BF3), the flow direction is vertical for this third folding phase, (g) Type 2 interference pattern or mirror- image patterns developed due to the interference between the second and third folds. The flow direction is E-W horizontal for this third folding phase.

the basement were metamorphosed and welded together during the first folding; the rock package became resistant to simple shear deformation and was replaced by pure shear deformation during the second folding phase (Naha et al., 1984, 1987). Several thrusts were developed during the second folding event (DF2, AF2, and BF2 thrusts), which strikes parallel to the axial plane and dips steeply to the NW or SE (Din, 2000). Progressive shortening produced axis parallel extension and lateral flow of the material and the thrusts underwent strike-slip tectonics. Down-dip stretching lineations were overprinted by horizontal stretching lineation or at places, the lineations were absent as the two strains nullified each other (Bhattacharyya et al., 1995; Roy, 1995; Dasgupta et al., 2012; Ruj and Dasgupta, 2014; Tiwari and Biswal, 2019) and in addition, conjugate strike-slip faults were produced.

The third fold occurs in a polyclinal fashion with multiple axial planes having strikes in NW-SE, E-W, and NE-SW directions. Using the axial plane orientation of the conjugate folds, the compressional stress for the third fold was deduced to be in the NE-SW direction. This implies that the compression axis was at a right angle to that of the second fold and parallel to the orogen axis (Fig. 9f, g). Orogen parallel compression is attributed to stress relaxation along the orogen after cessation of second folding (Naha et al., 1984). This further explains why the extension experienced during the second folding phase was equilibrated by orogen parallel shortening. As part of maintaining equilibrium, gravity folds are also produced due to vertical shortening (Naha et al., 1987).

The above discussed compressional setting resulted from several episodes of subduction/collisional tectonics between the Bundelkhand Craton and Mewar Craton, and Marwar Craton (Synchanthavong and Desai, 1977; Sinha-Roy, 1988; Bhowmik and Dasgupta, 2012; Singh et al., 2021). Each phase brought about an orogeny resulting in the accretion of terranes to the mobile belt. The terranes were juxtaposed parallelly in the NE-SW direction, which implies that the polarity of subduction was the same for the three terranes. The inferred direction of subduction is towards the NW, which comes the from the fact that the younger terranes were accreted towards the NW (Fig. 1d) and that arc magmatism (Sendra-Ambaji, Erinpura, and Sewariya granites) occurred in the NW (Singh et al., 2021). Based on the age of Berach granite, the Bhilwara orogeny has been interpreted to be ca. 2.6 Ga. The migmatisation in the Aravalli Terrane, intrusion of granulites in the Sandmata Complex, the Aravalli orogeny is constrained at 1.7–0.96 Ga which was coeval with North-Delhi orogeny (1.8–0.96 Ga) (Table 2). The Sewariya and Ambaji granite and fluid flow along the DS2 shear zones assigned 0.87 to 0.6 Ga for South Delhi orogeny (Singh et al., 2021) (Table 2). The Great Boundary Fault, the Rakhabdev shear zone, and the Kaliguman shear zone (Fig. 1b) probably mark the paleo-sutures of the subduction zones of these terranes.

3.3. Structural distinction between terranes

Deformation structures are often used to distinguish the terranes in a mobile belt. It has been previously interpreted that Aravalli Terrane is distinct from the SDT by having E-W trending AF1 folds. Further, scientist postulate that the AF2 and DF2 folds are contemporaneous and the DF2 fold has overprinted the Aravalli rocks as the AF2 fold (Naha et al., 1984). This interpretation was reasonable in the synclinorium model of the ADMB (Fig. 1c) as proposed by Heron (1953), but with the advent of geochronological data related to folding the above interpretation lost its edge. With more areas being covered by structural geological mapping, it became clear that the *E*-W AF1 folds are absent in many parts of the Aravalli Terrane and that the E-W DF1 folds are present in limited spots in SDT, at Bar and Babra. Therefore, we argue that the first E-W folding phase in the eastern part of the Aravalli Terrane and the linear volcano-sedimentary belts of Mangalwar Complex are the results of the rheological contrast between the basement and the rock cover, which led to larger strain concentration and rotation of N*E*-SW fold to E-W direction. Secondly, the superposition of DF2 folds as AF2 in the Aravalli terrane is beyond valid reasoning because of the difference in ages of Aravalli (1.7–0.96 Ga) and South Delhi orogenies (0.87–0.6 Ga) (Table 2). The Godhra granite marking the end of Aravalli orogeny (*syn*-AF3 folding) is ca. 0.96 Ga while the Ambaji granite (G1 granite, Singh et al., 2010) and Sewariya granite (Singh et al., 2021) marking the beginning of Delhi orogeny (syn-DF1 folding) is 0.87 Ga (Table 2).

Despite the gap in the orogenic period between the SDT and Aravalli terranes, thermal events related to the Delhi orogeny have overprinted the Aravalli Terrane as well as the basement rocks through thermal rejuvenation. The exact signature of deformation related to such thermal rejuvenation in the older terranes is still a matter of debate. It is, by and large, attributed to the reactivation of pre-existing shear zones and faults by late-stage brittle deformation in older terranes (Bhardwaj and Biswal, 2019; Tiwari and Biswal, 2019; Singh et al., 2021). During reactivation, hydrothermal fluids passed through the brittle fractures and altered the country rock. In the process, sulfide minerals are also deposited (Sharma and Biswal, 2020; Sharma et al., 2022). Groundwater flow through brittle fractures created structural aquifers bringing rock-water interaction (Pradhan et al., 2021, 2022). These low to medium temperature alterations probably reset the geochronological ages (monazite ages) of the older terrane. The primary monazite grains were reprecipitated and assumed spongy nature (Tiwari and Biswal, 2019; e.g. Behera et al., 2019; Schulz, 2021). Those neograins provide younger ages related to the fluid activity.

3.4. Exhumation of mid-lower crustal rocks

The ADMB is dominated by low- to medium-grade metamorphic rocks. Granulite occurs in limited areas of Sandmata Complex, and in the SDT near Ambaji, which were exhumed from the mid-lower crust and emplaced within the low-grade belts at different period of time. The DF2-BF2 thrusts were the main channel for exhumation. Further, Beawar gneiss, Anasagar gneiss, Bar-Babra conglomerate, and Todgarh-Srinagar conglomerate were also thrusted up to the upper sequence of SDT at 0.8 Ma (Table 2). The thrusts were generated by the same compressional stress as that of the DF1 and DF2 folds. The Sandmata granulite was exhumed at ca 1.7 Ga (Table 2). After the exhumation of the rocks to the brittle-ductile transition zone, the rheological contrast between the middle and upper crust led to lateral extrusion of material exemplifying escape tectonics (Tiwari et al., 2020b). Subsequently, extensional faulting and erosion exposed them to the surface. It has been explained in earlier sections that tilting of the Aravalli- and Bhilwara Terrane to the south of the Banas shear zone might have contributed additionally to the exposure of the lower crustal rocks in northern blocks. Further, the normal faulting in the SDT near Babra has also exposed the basement rocks near Pilwa and Chinwali areas.

3.5. Indentation tectonics and analogy with other orogens

The general model explaining the extrusion of lithospheric blocks in the Tibet Plateau involves the indentation tectonics at Nanga Parbat. The convergence between India and Asia created a syntaxial bend close to the indenter and the extreme shortening at the bend was accommodated by lateral extrusion of the blocks through strike-slip faults. The Karakoram fault is one of the faults that developed at the edge of the indenter. In addition, there are several strike-slip faults in the Tibet Plateau. While the lithospheric blocks bounded by the strike-slip faults undergo minor crustal deformation, the strike-slip fault zones experience transpressional strain. This is defined as escape tectonics (Tapponnier et al., 1982; Deng et al., 2014). Further, lateral extrusion created several high-angle normal faults due to orogen parallel extension (Hintersberger et al., 2010; Liu et al., 2012). Gravitation collapse of the orogen also adds to lateral escape of the material as explained for the escape tectonics for Anatolia block in the eastern Mediterranean sector (Dhont et al., 2006). Escape tectonics are widely observed in Phanerozoic orogens, but less preserved in the Precambrian orogen owing to a

deeper level of erosion. However, there are reports of escape tectonics in proto-Kalahari craton (Jacobs et al., 1993), East African Antarctic orogen (Jacobs and Thomas, 2004) and Pilbara-Gawler craton (Krapez, 1999).

In the ADMB, the Berach granite and its precursor acted as the promontory/indentor on the frontal part of the Bundedkhand and Mewar Craton, which created a syntaxial bend in the eastern part of the orogen. All features of the escape tectonics resulting from the indentation are not preserved since the middle-lower part of the ADMB has been exposed at present. The arch angle of the syntaxis gradually flattens out from the source region, near the contact of Berach granite, towards the west, and the outer SDT remains almost straight with extreme shortening at the centre and fanning out on both ends. The shear zone pairs namely the Phulad shear zone, with the Kaliguman shear zone, the Kaliguman shear zone with the Delwara shear zone, the Delwara shear zone with the Jahazpur thrust, the Jahazpur thrust with the Great boundary fault which all show narrow mutual separation towards the hinge of the syntaxial bend (Fig. 1b). The sub-horizontal gliding planes as seen in modern fold-thrust belts are missing in the ADMB as the thrusts have passed from gentler to steeper attitude at depth (e.g. Ramsay and Huber, 1987). However, NW and SE synclines of SDT near Beawar represent thrust belts (Fig. 2). Thrusts that are divergent with the central line located at the Beawar gneiss, resembling pro-and retro wedge thrusts of the modern orogen. Near the Ajmer fold-and-thrust belts are reported. Granulite near Ambaji is marked by thrust belts (Fig. 4). The volcano-sedimentary belts within the Mangalwar Complex (Fig. 9) are marked by thrust belts. The Aravalli terrane shows thrust belts on either side of the Sarada inlier (Fig. 7). At several places, these thrusts are subsequently overprinted by strike-slip tectonics. The thrusts lying on the NE limb of the syntaxis near Beawar and within the Mangalwar Complex show a dextral sense of shearing. The Ambaji granulite that lies in the SW limb of the syntaxis show sinistral shearing along the strike-slip faults. The Banas shear zone occurs on the syntaxis shoulder. The crustal blocks bounded by such strike-slip faults do not show much deformation during the lateral escape, as they behaved as rigid blocks. The fault zones show the transpressional strain. In addition, the ADMB is cross-cut by high angle normal faults at several places attributed to the extension of the mobile belt due to lateral extrusion. The present geometry of the syntaxis is assigned to *syn*-South Delhi orogeny and the effect of indentation during Bhilwara and Aravalli orogeny requires more structural and geochronological work.

3.6. Supercontinent correlation

The Aravalli and South Delhi orogens formed over the basement of the Bhilwara Terrane which was stabilized at 2.6 Ga during Bhilwara orogeny. The intrusion of 2.6 Ga old granites has been observed in several parts of the Indian Shield that suggest uniformity in the evolution of the Indian Shield during the Precambrian period. The Aravalli-North Delhi Terrane and South Delhi Terrane along with contemporary mobile belts in Peninsular India helped in the reconstruction of the Paleoproterozoic Columbia and Neoproterozoic Gondwanaland Supercontinents. The Aravalli orogen (1.7 to 0.96 Ga) and the Sausar orogen in Central India (ca. 2.1 to 0.9 Ga, Mohanty, 2021) were correlated with the Xiong'er belt of North China Craton (1.78 to 1.45 Ga) and Capricorn orogen in Australia in the reconstruction of Columbia Supercontinent (Zhao et al., 2002, 2009; Mohanty, 2021; Banerjee et al., 2021). Hence, North China Craton is plotted outboard of the Columbia Supercontinent close to India. In another correlation, India is juxtaposed against Sarmatia of Baltica at 1.4 Ga (Pisarevsky et al., 2013). The South Delhi orogen is juxtaposed against the Arabian-Nubian shield (Collins and Pisarevsky, 2005), Madagascar (Singh et al., 2010), and the Yangtze and Cathaysia blocks of South China (Wang et al., 2017; Zhao et al., 2018) in the Neoproterozoic Gondwanaland Supercontinent assembly. The present synthesis of structural-geochronological data will further help in fine-tuning such correlation.

4. Conclusions

The collation of structural geological studies of the ADMB leads us to the following conclusion:

a. The Precambrian ADMB is characterized by accretion of low- to medium grade metamorphic terranes successively towards the NW, the Bhilwara (Archean), Aravalli (Paleoproterozoic), North Delhi (Paleoproterozoic) and South Delhi (Meso-Neoproterozoic), which owe their origin initially to extensional tectonics followed by compressional tectonics at different times (Table 2). Compressional tectonics is the result of subduction/collision similar to Phanerozoic plate tectonics. Individual terranes show the uniform polarity of subduction, as a result, the folds and shear zones show a similar trend though they developed during different periods. Coaxial folding along the NE-SW axis between the first two phases of folding (type 3 interference pattern) is the major deformation structure in each of these terranes. The first fold (DF1, NF1, AF1, BF1) is isoclinal and recumbent and the second fold (DF2, NF2, AF2, BF2) is upright with the NE-SW axial plane. The NE-SW trend of the mobile belt is primarily due to second folding. The third fold (DF3, NF3, AF3, BF3) is along the NW-SE axial plane and has produced dome- and basin-interference structures with the folds of the second folding phase. The folds are developed at different periods as shown in Table 2.
b. The eastern part of the Aravalli Terrane and the volcano-sedimentary belts in the Mangalwar Complex reveals that the basement gneisses are involved in folding phases. Due to the rheological contrast, the NE-SW trending AF1 folds have turned into E-W direction with progressive decoupling between the basement and rock cover. In those cases, AF2 folding has curved the hinge of the AF1 fold. Hence, E-W folding is not a distinguishing structure of the Aravalli Terrane. Further, the third folding phase in the mobile belt (DF3, NF3, AF3, BF3) has vertical flow even though they are developed in different periods (Table 2). In the case where the third fold is associated with strike-slip axial planar shear, the flow turned to horizontal and the second fold axial plane folded around the third fold producing a mirror image pattern. This has created the swinging orientation of the mobile belt between NE-SW to E-W direction, as in the case of the Zawar, Champaner, and Ambaji areas.
c. The second folding phase is associated with several longitudinal thrusts striking parallel to that of the axial plane of the second fold. These thrusts are responsible for the exhumation of mid-lower crustal rocks. The granulites of Sandmata, Ambaji, the Beawar gneiss, the Anasagar gneiss, basal conglomerates of the Bar and Srinagar area are emplaced into the upper crust due to such thrusting. Thrusting of the Sandmata granulite is earlier than that of the Ambaji granulite (Table 2). The thrusts contain several kinematic indicators including porphyroclasts, S—C fabric, and asymmetric folds. The kinematic vorticity number indicates transpressive strain. The thrusts are overprinted by strike-slip shearing.
d. The mobile belt has undergone indentation tectonics during syn-Delhi deformation, with the Berach granite acting as the indenter in the collisional front between the Bundelkhand Craton and Marwar Craton. The SDT shows the lateral escape of material through strike-slip faulting due to strain concentration close to the syntaxial bend.
e. The Aravalli terrane with Columbia Supercontinent and South Delhi terrane with Gondwanaland Supercontinent have been correlated.

Declaration of Competing Interest

The authors declare that they have no conflict of interest.

Acknowledgments

We are thankful to the Department of Earth Sciences, IIT Bombay for financial support to several Doctoral (Ph.D.) and Master's (M.Sc./M.

Tech.) degree students for their dissertation work on the structural geology of the mobile belt in different areas. The first author was an officer in the Geological Survey of India, before joining IIT Bombay, where he was engaged in mapping and structural studies of different parts of the orogen. Thanks to Ms. Ananya Ghosh and Ms. Vidushi Singh for their help in drawing some of the figures. We are thankful to Prof. Rajat Mazumder for inviting us to write the review paper, his valuable editorial comments, Prof. Douwe van Hinsbergen as handling editor, and anonymous reviewers for their critical comments and suggestions that immensely helped to improve the manuscript.

References

Ahmad, I., Mondal, M.E.A., 2016. Do the BGC-I and BGC-II domains of the Aravalli craton, northwestern India represent accreted terranes? Earth Sci. India 9, 167–175.
Anderson, J.B., 1999. Antarctic Marine Geology. Cambridge University Press.
Bakliwal, P.C., Ramasamy, S.M., 1987. Lineament fabric of Rajasthan and Gujarat, India. Rec. Geol. Surv. India 113, 54–64.
Banerjee, A., Sequeira, N., Bhattacharya, A., 2021. Tectonics of the Greater India Proterozoic Fold Belt, with emphasis on the nature of curvature of the belt in west-Central India. Earth-Sci. Rev. 221, 103758 https://doi.org/10.1016/j.earscirev.2021.103758.
Behera, B.M., Waele, B.D., Thirukumaran, V., Sundaralingam, K., Narayanan, S., Sivalingam, B., Biswal, T.K., 2019. Kinematics, strain pattern and geochronology of the Salem-Attur shear zone: Tectonic implications for the multiple sheared Salem-Namakkal blocks of the Southern Granulite terrane, India. Precambrian Res. 324, 32–61.
Bhardwaj, A., 2019. Structure, Geochemistry and Geochronology of Punagarh Basin and its Basement: Implications for Tectono-Thermal Evolution Of Trans- Aravalli Terrain, NW India. Ph. D. Thesis. IIT Bombay, 96pp.
Bhardwaj, A., Biswal, T.K., 2019. Deformation and tectonic history of Punagarh basin in the Trans-Aravalli Terrane of North-Western India. In: Mondal, M.E.A. (Ed.), Geological Evolution of the Precambrian Indian Shield. Springer, Cham., Switzerland, pp. 159–178.
Bhatnagar, S.N., Mathur, S.B., 1989. Geology of lead-zinc resources. In: Geology of Lead-Zinc Resources, 1-2. Hindzin Tech, pp. 15–28.
Bhattacharyya, T., Sengupta, S., Mukhopadhyay, D., 1995. Tectonic status of the Delhi-pre-Delhi contact, east of Beawar, Central Rajasthan. Mem Geol. Soc. India 31, 217–230.
Bhowmik, S.K., Dasgupta, S., 2012. Tectonothermal evolution of the Banded Gneissic complex in Central Rajasthan, NW India: present status and correlation. J. Asian Earth Sci. 49, 339–348.
Bhowmik, S.K., Dasgupta, S., Baruah, S., Kalita, D., 2018. Thermal history of a late mesoproterozoic paired metamorphic belt during Rodinia assembly: new insight from medium-pressure granulites from the Aravalli-Delhi mobile belt, northwestern India. Geosci. Front. 9, 335–354.
Biswal, T.K., 1988. Polyphase deformation in Delhi rocks, southeast of Amirgad, Banaskantha district of Gujarat. Geol. Soc. India Mem. 7, 267–277.
Biswal, T.K., 1993. Structural history of Barotia Group near Bar, Pali district of Rajasthan. Indian Min. 47, 123–130.
Biswal, T.K., Nayak, S., Harish, T.R., Unikrishnan, S., 1997. Evidence of ductile shearing from the extensional crenulation cleavage: an example from Zawar area, the Aravalli mountain. Curr. Sci. 73, 701–703.
Biswal, T.K., Gyani, K.C., Parthasarathy, R., Pant, D.R., 1998a. Implications of the geochemistry of the pelitic granulites of the Delhi supergroup, Aravalli Mountain Belt, northwestern India. Precambrian Res. 87, 75–85.
Biswal, T.K., Gyani, K.C., Parthasarathy, R., Pant, D.R., 1998b. Tectonic implication of geochemistry of gabbronorite-basic granulite suite in the Proterozoic Delhi Supergroup, Rajasthan, India. J. Geol. Soc. India 52, 721–732.
Biswal, T.K., Sarkar, S., Pal, A., Chakraborty, U., 2004. Pseudotachylites of the Kui-Chitraseni shear zones of the Precambrian Aravalli Mountain, Rajasthan. J. Geol. Soc. India 64, 325–335.
Chander, S., Bhattacharjee, S., Roy Choudhury, M., Agarwal, N., 2021. Characterisation of Kalalikhera felsic volcanics, Pur-Banera belt, Rajasthan: Insights from monazite–xenotime geochemistry and chemical ages. J. Earth Syst. Sci. 130, 84. https://doi.org/10.1007/s12040-021-01572-8.
Choudhary, A.K., Gopalan, K., Sastry, C.A., 1984. Present status of the geochronology of the Precambrian rocks of Rajasthan. Tectonophysics 105, 131–140.
Choudhury, M.R., Das, S., Chatterjee, S.M., Sengupta, S., 2016. Deformation of footwall rock of Phulad Shear Zone, Rajasthan: evidence of transpressional shear zone. J. Earth Syst. Sci. 125, 1033–1040.
Chowdhury, A., Bosevska, L., 2017. Strain Analysis in Rock Group of Pur-Basin, India. J. Geol. Geogr. Geoecol. 25, 23–37.
Collins, A.S., Pisarevsky, S.A., 2005. Amalgamating eastern Gondwana: the evolution of the Circum-Indian Orogens. Earth-Sci. Rev. 7, 229–270.
Coulson, A.L., 1933. The geology of Sirohi state, Rajputana. Mem. Geol. Surv. India 63, 1–166.
Crawford, A.R., 1970. The Precambrian geochronology of Rajasthan and Bundelkhand, northern India. Can. J. Earth Sci. 7, 91–110.
Das, A.R., 1988. Geometry of the superposed deformation in the Delhi Supergroup of rocks, north of Jaipur, Rajasthan. In: Roy, A.B. (Ed.), Precambrian of the Aravalli Mountain, Rajasthan India, Geol. Soc. India Mem, vol. 7, pp. 247–266.
Dasgupta, S.C., 1982. Superposed folding in the Precambrians of the Pur area, Bhilwara district of Rajasthan. Quart. Jour. Geol. Min. Soc. India 54, 1–17.
Dasgupta, N., Mukhopadhyay, D., Bhattacharyya, T., 2012. Analysis of superposed strain: a case study from Barr Conglomerate in the South Delhi Fold Belt, Rajasthan, India. J. Struct. Geol. 34, 30–42.
De Wall, H., Pandit, M.K., Chauhan, N.K., 2012. Paleosol occurrences along the Archean–Proterozoic contact in the Aravalli craton, NW India. Precambrian Res. 216, 120–131.
De Wall, H., Pandit, M.K., Sharma, K.K., Schöbel, S., Just, J., 2014. Deformation and granite intrusion in the Sirohi area, SW Rajasthan—Constraints on Cryogenian to Pan-African crustal dynamics of NW India. Precambrian Res. 254, 1–18.
Deb, M., 2000. VMS deposits: Geological characteristics, genetic models and a review of their metallogenesis in the Aravalli range, NW India. In: Deb, M. (Ed.), Crustal Evolution and Metallogeny in the Northwestern Indian Shield. Narosa Publishing House, New Delhi, pp. 329–362.
Deb, M., Thorpe, R.I., Cumming, G.L., Wagner, P.A., 1989. Age, source and stratigraphic implications of Pb isotope data for conformable, sediment-hosted, base metal deposits in the Proterozoic Aravalli-Delhi orogenic belt, northwestern India. Precambrian Res. 43, 1–22.
Deb, M., Thorpe, Ralph, Krastic, Dragan, 2002. Hindoli group of rocks in the eastern fringe of the aravalli-delhi orogenic belt-archean secondary greenstone belt or proterozoic supracrus tals? Gondwana Res. 5, 879–883.
Deng, Y., Panza, G.F., Zhang, Z., Romanelli, F., Ma, T., Doglioni, C., Wang, P., Zhang, X., Teng, J., 2014. Transition from continental collision to tectonic escape? A geophysical perspective on lateral expansion of the northern Tibetan Plateau. Earth Planets Space 66, 1–10.
Desai, S.J., Patel, M.P., Merh, S.S., 1978. Polymetamorphites of Balamar-Abu Road area, north Gujarat and southwestern Rajasthan. J. Geol. Soc. India 19, 383–394.
Dey, B., Das, K., Dasgupta, N., Bose, S., Hidaka, H., Ghatak, H., 2019. Zircon U–Pb (SHRIMP) ages of the Jahazpur Granite and Mangalwar Gneiss from the Deoli-Jahazpur Sector, Rajasthan, NW India: A preliminary reappraisal of stratigraphic correlation and implications to crustal growth. In: Mondal, M.E.A. (Ed.), Geological Evolution of the Precambrian Indian Shield, Society of Earth Scientists Series, pp. 39–56. https://doi.org/10.1007/978-3-319-89698-4_3.
Dhont, D., Chorowicz, J., Luxey, P., 2006. Anatolian escape tectonics driven by Eocene crustal thickening and Neogene–Quaternary extensional collapse in the eastern Mediterranean region. In: Dilek, Y., Pavlides, S. (Eds.), Postcollisional Tectonics and Magmatism in the Mediterranean Region and Asia, Geol. Soc. Am. Spec. Papers, vol. 409, pp. 441–462.
Din, S.U., Iqbaluddin, 2000. Thrust controlled lineament of the Aravalli Delhi fold belt, Rajasthan, India, Mapped from Landsat TM image. J. Indian Soc. Remote Sens. 28, 47–58.
D'Souza, J., Prabhakar, N., Xu, Y., Sharma, K.K., Sheth, H., 2019. Mesoarchaean to Neoproterozoic (3.2–0.8 Ga) crustal growth and reworking in the Aravalli Craton, northwestern India: Insights from the Pur-Banera supracrustal belt. Precambrian Res. 332, 105383 https://doi.org/10.1016/j.precamres.2019.105383.
D'Souza, J., Sheth, H., Xu, Y., Wegner, W., Prabhakar, N., Sharma, K.K., Koeberl, C., 2020. Neoarchaean crustal reworking in the Aravalli Craton: Petrogenesis and tectonometamorphic history of the Malola granite, Bhilwara area, northwestern India. Geol. J. 55 (12), 8186–8210.
D'Souza, J., Prabhakar, N., Sheth, H., Xu, Y., 2021. Metamorphic P–T–t–d evolution of the Mesoproterozoic Pur-Banera supracrustal belt, Aravalli Craton, northwestern India: Insights from phase equilibria modelling and zircon–monazite geochronology of metapelites. J. Metamorph. Geol. 39 (9), 1173–1204.
Dutta, R., Bhu, H., Purohit, R., Sharma, K.K., 2021. Geology of granitoids of Pindwara–Abu Road Belt from Mesoproterozoic Delhi Supergroup: Tectonic implications. J. Earth Syst. Sci. 130, 1–17.
Fareeduddin, Kroner, 1998. Single zircon age constraints on the evolution of Rajasthan granulite. In: Paliwal, B.S. (Ed.), The Indian Precambrian. Scientific Publishers (India), Jodhpur, pp. 547–556.
Fareeduddin, M., Basavalingu, B., Janardhan, A., 1994. PT conditions of pelitic granulites and associated charnockites of Chinwali area, west of Delhi fold belt, Rajasthan. J. Geol. Soc. India 43, 169–178.
Fossen, H., 2010. Structural Geology. Cambridge University Press.
Gandhi, S.M., Paliwal, H.V., Bhatnagar, S.N., 1984. Geology and ore reserve estimates of Rampura-Agucha zinc-lead deposit, Bhilwara district, Rajasthan. J. Geol. Soc. India 25, 689–705.
Gangopadhyay, P.K., 1967. Structural framework of Alwar region with special reference to the occurrence of some rock types. In: Proc. Symp. Upper Mantle Project, NGRI, Hyderabad, pp. 420–429.
Ghosh, S.K., Ramberg, H., 1976. Reorientation of inclusions by combination of pure shear and simple shear. Tectonophysics 34, 1–70.
Gopalan, K., Trivedi, J.R., Merh, S.S., Patel, P.P., Patel, S.G., 1979. Rb-Sr age of Godhra and related granites, Gujarat, India. In: Proc. Indian Acad. Sci. Section A. Part 2, Earth and Planet. Sci, 88, pp. 7–17.
Goyal, N., Sharma, P.K., Allipeera, P., Yadav, G.S., Yadav, O.P., Nanda, L.K., Parihar, P. S., 2013. Integration of geological and geophysical data: a guide to exploration for uranium in Raghunathgarh area, North Delhi fold belt, Rajasthan. J. Appl. Geochem. 15, 289–301.
Gregory, L.C., Meert, J.G., Bingen, B., Pandit, M.K., Torsvik, T.H., 2009. Paleomagnetism and geochronology of the Malani Igneous Suite, Northwest India: implications for the configuration of Rodinia and the assembly of Gondwana. Precambrian Res. 170, 13–26.
Guha, D.B., Bhattacharya, A.K., 1995. Metamoprhic evolution and high grade reworking of the Sandmata complex granulites. Mem. Geol. Soc. India 31, 163–198.
Gupta, B.C., 1934. The geology of central Mewar. Mem. Geol. Surv. India 65, 107–169.

Gupta, S.N., Arora, Y.K., Mathur, R.K., Iqbaluddin, B.P., Sahai, T.N., Sharma, S.B., Murthy, M.V.N., 1980. Lithostratigraphic Map of Aravalli region, Southern Rajasthan and Northeastern Gujarat. Geological Survey of India, Hyderabad.
Gupta, S.N., Arora, Y.K., Mathur, R.K., Iqbaluddin, B.P., Sahai, T.N., Sharma, S.B., 1997. The Precambrian geology of the Aravalli region, southern Rajasthan and north eastern Gujarat. Mem. Geol. Surv. India 123, 262pp.
Gupta, P., Guha, D.B., Chattopadhyay, B., 1998. Basement-cover relationship in the Khetri copper belt and the emplacement mechanism of the granite massifs, Rajasthan, India. J. Geol. Soc. India 52, 417–432.
Hahn, G., Kodl, G., De Wall, H., Schulz, B., Bestmann, M., Chauhan, N.K., 2020. Deformation in the Aravalli supergroup, Aravalli-Delhi Mobile Belt, NW India and Tectonic significance. In: Biswal, T.K., et al. (Eds.), Structural Geometry of Mobile Belts of the Indian Subcontinent, Society of Earth Scientists Series. Springer Nature, Switzerland AG, pp. 23–55. https://doi.org/10.1007/978-3-030-40593-9_2.
Hatui, K., Chattopadhyay, A., 2020. Modification of pre-existing folds in a shear zone: A case study from Kumbhalgarh–Ranakpur area, South Delhi Fold Belt, Rajasthan, India. J. Earth Syst. Sci. 129, 1–16.
Heron, A.M., 1953. The geology of central Rajputana. Mem. Geol. Surv. India 79, 389.
Heron, A.M., Ghosh, P.K., 1938. The geology of Palanpur, Danta and parts of Idar state. Rec. Geol. Surv. India 72, 367–412.
Hintersberger, E., Thiede, R.C., Strecker, M.R., Hacker, B.R., 2010. East-west extension in the NW Indian Himalaya. Bulletin 122, 1499–1515.
Holmes, A., 1955. Dating the precambrian of peninsular India and Ceylon. Proc. Geol. Assoc. Can. 7, 81–106.
Jacobs, J., Thomas, R.J., 2004. Himalayan-type indenter-escape tectonics model for the southern part of the late Neoproterozoic–early Paleozoic East African–Antarctic orogen. Geology 32, 721–724.
Jacobs, J., Thomas, R.J., Weber, K., 1993. Accretion and indentation tectonics at the southern edge of the Kaapvaal craton during the Kibaran (Grenville) orogeny. Geology 21, 203–206.
Joshi, A.U., 2019. Structural Evolution of Precambrian Rocks of Champaner Group, Gujarat, Western India. Unpublished Ph.D. Thesis. The Maharaja Sayajirao University of Baroda, 190pp.
Joshi, A.U., Limaye, M.A., 2020. Anisotropy of Magnetic Susceptibility (AMS) Studies on Quartzites of Champaner Group, Upper Aravallis. In: Biswal, T.K., et al. (Eds.), Structural Geometry of Mobile Belts of the Indian Subcontinent, Society of Earth Scientists Series. Springer Nature, Switzerland AG, pp. 199–211. https://doi.org/10.1007/978-3-030-40593-9_9.
Just, J., Schulz, B., De Wall, H., Jourdan, F., Pandit, M.K., 2011. Monazite CHIME/EPMA dating of Erinpura granitoid deformation: Implications for Neoproterozoic tectono-thermal evolution of NW India. Gondwana Res. 19, 402–412.
Kaur, P., Chaudhri, N., Raczek, I., Kröner, A., Hofmann, W., 2009. Record of 1.82 Ga Andean-type continental arc magmatism in NE Rajasthan, India: Insights from zircon and Sm–Nd ages, combined with Nd–Sr isotope geochemistry. Gondwana Res. 16, 56–71.
Kaur, P., Zeh, A., Chaudhri, N., Gerdes, A., Okrusch, M., 2013. Nature of magmatism and sedimentation at a Columbia active margin: insights from combined U–Pb and Lu–Hf isotope data of detrital zircons from NW India. Gondwana Res. 23, 1040–1052.
Kaur, P., Zeh, A., Chaudhri, N., 2017. Palaeoproterozoic continental arc magmatism, and Neoproterozoic metamorphism in the Aravalli-Delhi orogenic belt, NW India: New constraints from in situ zircon U-Pb-Hf isotope systematics, monazite dating and whole-rock geochemistry. J. Asian Earth Sci. 136, 68–88.
Kaur, P., Zeh, A., Chaudhri, N., Tiwana, J.K., 2020. First evidence of late paleoproterozoic/early mesoproterozoic sediment deposition and magmatism in the central Aravalli orogen (NW India). J. Geol. 128, 109–129.
Kaur, P., Zeh, A., Chaudhri, N., 2021. Archean to Proterozoic (3535–900 Ma) crustal evolution of the central Aravalli Banded Gneissic Complex, NW India: New constraints from zircon U-Pb-Hf isotopes and geochemistry. Precambrian Res. 359, 106179 https://doi.org/10.1016/j.precamres.2021.106179.
Khan, M.S., Smith, T.E., Raza, M., Huang, J., 2005. Geology, geochemistry and tectonic significance of mafic-ultramafic rocks of Mesoproterozoic Phulad ophiolite suite of South Delhi fold belt, NW Indian Shield. Gondwana Res. 8, 553–566.
Knight, J., Lowe, J., Joy, S., Cameron, J., Merrillees, J., Nag, S., Shah, N., Dua, G., Jhala, K., 2002. The Khetri copper belt, Rajasthan: Iron oxide copper-gold terrane in the Proterozoic of NE India. In: Porter, T.M. (Ed.), Hydrothermal Iron Oxide Copper-Gold and Related Deposits: A Global Perspective, v. 2, PGC Adelaide, pp. 321–341.
Krapez, B., 1999. Stratigraphic record of an Atlantic-type global tectonic cycle in the Paleoproterozoic Ashburton province of Western Australia: Australian. J. Earth Sci. 46, 71–87.
Kröner, A., Stern, R.J., 2005. AFRICA | Pan-African Orogeny. In: Selley, R.C., et al. (Eds.), Encyclopedia of Geology. Elsevier, pp. 1–12.
Kumar, H., Pandit, M., 2020. Recurrent seismicity in Rajasthan State in the tectonically stable NW Indian Craton. J. Earth Sci. 12, 1–9.
Kumar, A., Prakash, A., Saha, L., Corfu, F., Bhattacharya, A., 2019. 940 Ma anatexis in 1726 Ma orthogneiss in the northern margin of the Bhilwara belt and significance for the Precambrian evolution in Northwest India. J. Geol. 127, 627–641.
Lal, R.K., Shukla, R.S., 1975. Genesis of cordierite-gedrite-cummingtonite rocks of the northern portion of the Khetri copper belt, Rajasthan, India. Lithos 8, 175–186.
Liu, X., Liu, X., Leloup, P.H., Maheo, G., Paquette, J.L., Zhang, X., Zhou, X., 2012. Ductile deformation within Upper Himalaya crystalline sequence and geological implications, in Nyalam area, southern Tibet. Chin. Sci. Bull. 57, 3469–3481.
MacDougall, J.D., Gopalan, K., Lugmair, G.W., Roy, A.B., 1983. The Banded Gneissic complex of Rajasthan, India: early crust from depleted mantle at 3.5 AE? EOS Trans. Am. Geophys. Union 64, 351.
Mahadani, T., Biswal, T.K., Mukherjee, T., 2015. Strain estimation of folds, orbiculites and quartz phenocrysts in the Ambaji Basin of the South Delhi Terrane, Aravalli-Delhi Mobile Belt, NW India and its Tectonic implication. J. Geol. Soc. India 85, 139–152.
Mamtani, M.A., Greiling, R.O., 2005. Granite emplacement and its relation with regional deformation in the Aravalli Mountain Belt (India)-inferences from magnetic fabric. J. Struct. Geol. 27, 2008–2029.
Mamtani, M.A., Karmakar, B., Merh, S.S., 2002. Evidence of polyphase deformation in gneissic rocks around Devgadh Bariya: implications for evolution of Godhra Granite in the southern Aravalli region (India). Gondwana Res. 5, 401–408.
Mehdi, M., Kumar, S., Pant, N.C., 2015. Low grade metamorphism in the Lalsot-Bayana Sub-basin of the North Delhi Fold Belt and its tectonic implication. J. Geol. Soc. India 85, 397–410.
Mishra, B., Kumar, K., Khandelwal, M.K., Nanda, L.K., 2018. Uranium mineralization in the Khetri Sub-Basin, North Delhi Fold Belt, India. No. IAEA-CN-261, pp. 285–288.
Misra, A., Chauhan, A., Chatterjee, D., 2020. Petrology, geochemistry and geochronology of neoarchean A-type granite from Alwar basin, north Delhi terrane, NW India. J. Earth Syst. Sci. 129, 1–34.
Mohanty, S.P., 2021. The Bastar Craton of Central India: Tectonostratigraphic evolution and implications in global correlations. Earth-Sci. Rev. 221, 103770 https://doi.org/10.1016/j.earscirev.2021.103770.
Mukhopadhyay, D., Dasgupta, S., 1978. Delhi Pre-Delhi relations near Badnor, central Rajasthan. Indian J. Earth Sci. 5, 183–190.
Mukhopadhyay, D., Bhattacharyya, T., Chattopadhyaya, N., Robert, L., Tobisch, O.T., 2000. Anasagar gneiss: a folded granitoid pluton in the Proterozoic South Delhi Fold Belt, Central Rajasthan. Proc. Indian Acad. Sci. 109, 21–37.
Mukhopadhyay, D., Chattopadhyay, N., Bhattacharyya, T., 2010. Structural evolution of a gneiss dome in the axial zone of the Proterozoic South Delhi Fold Belt in Central Rajasthan. J. Geol. Soc. India 75, 18–31.
Naha, K., Chaudhuri, A.K., 1968. Large scale fold interference in a metamorphic-migmatitic complex. Tectonophysics 6, 127–142.
Naha, K., Halyburton, R.V., 1974. Early Precambrian stratigraphy of central and southern Rajasthan, India. Precambrian Res. 1, 55–73.
Naha, K., Halyburton, R.V., 1977. Structural pattern and strain history of a superposed fold system in the Precambrian of central Rajasthan, India. II. Strain history. Precambrian Res. 4, 85–111.
Naha, K., Mohanty, S., 1988. Response of basement and cover rocks to multiple deformations: a study from the Precambrian of Rajasthan, western India. Precambrian Res. 42, 77–96.
Naha, K., Mukhopadhyay, D.K., Mohanty, R., Mitra, S.K., Biswal, T.K., 1984. Significance of contrast in the early stages of the structural history of the Delhi and the pre-Delhi rock groups in the Proterozoic of Rajasthan, western India. Tectonophysics 105, 193–206.
Naha, K., Mitra, S.K., Biswal, T.K., 1987. Structural history of the rocks of the Delhi Group around Todgarh, Central Rajasthan. Indian J. Geol. 59, 126–156.
Pandit, M.K., Carter, L.M., Ashwal, L.D., Tucker, R.D., Torsvik, T.H., Jamtveit, B., Bhushan, S.K., 2003. Age, petrogenesis and significance of 1 Ga granitoids and related rocks from the Sendra area, Aravalli Craton, NW India. J. Asian Earth Sci. 22, 363–381.
Pant, N.C., Kundu, A., Joshi, S., 2008. Age of metamorphism of Delhi Supergroup rocks-electron microprobe ages from Mahendragarh district, Haryana. J. Geol. Soc. India 72, 365–372.
Passchier, C.W., 1987. Stable positions of rigid objects in non-coaxial flow—a study in vorticity analysis. J. Struct. Geol. 9, 679–690.
Pisarevsky, S.A., Biswal, T.K., Wang, X.-C., De Waele, B., Ernst, R., Söderlund, U., Tait, J. A., Ratre, K., Singh, Y.K., Cleve, M., 2013. Palaeomagnetic, geochronological and geochemical study of mesoproterozoic lakhna dykes in the bastar craton, India: implications for the mesoproterozoic supercontinent. Lithos 174, 125–143.
Pradhan, R.M., Guru, B., Pradhan, B., Biswal, T.K., 2021. Integrated multi-criteria analysis for groundwater potential mapping in Precambrian hard rock terranes (North Gujarat), India. Hydrol. Sci. J. 66, 961–978.
Pradhan, R.M., Behera, A.K., Kumar, S., Kumar, P., Biswal, T.K., 2022. Recharge and Geochemical Evolution of Groundwater in Fractured Basement Aquifers (NW India): Insights from Environmental Isotopes ($\delta^{18}O$, $\delta^{2}H$, and ^{3}H) and Hydrogeochemical Studies. Water 14 (3), 315. https://doi.org/10.3390/w14030315.
Prakash, I., Gupta, K.S., Dey, A., Singh, P.K., Dhote, P.S., Basheer, H.S., Daliya, A., Modi, V.S., 2012. Geology and mineral resources of Gujarat, Daman and Diu. Geol. Surv. India 1–102.
Prakash, D., Kumar, M., Rai, S.K., Singh, C.K., Singh, S., Yadav, R., Jaiswal, S., Srivastava, V., Yadav, M.K., Bhattacharjee, S., Singh, P.K., 2021. Metamorphic P–T evolution of Hercynite-quartz-bearing granulites from the Diwani Hill, North East Gujarat (NW India). Precambrian Res. 352, 105997 https://doi.org/10.1016/j.precamres.2020.105997.
Purohit, R., Bhu, H., Sarkar, A., Ram, J., 2015. Evolution of the ultramafic rocks of the Rakhabdev and Jharol belts in southeastern Rajasthan, India: New evidence from imagery mapping, petro-minerological and OH stable isotope studies. J. Geol. Soc. India 85, 331–338.
Raja Rao, C.S., Poddar, B.C., Basu, K.K., Dutta, A.K., 1971. Precambrian stratigraphy of Rajasthan: a review. Rec. Geol. Surv. India 101, 60–71.
Ramsay, J.G., 1967. Folding and Fracturing of Rocks. McGraw-Hill Book, New York.
Ramsay, J.G., Huber, M.I., 1987. The Techniques of Modern Structural Geology: Folds and Fractures, vol. 2. Academic Press, London.
Ramsay, J.G., Lisle, R.J., 2000. The Techniques of Modern Structural Geology: Applications of Continuum Mechanics in Structural Geology, vol. 3. Academic Press, London.
Ray, S.K., 1974a. Structural history of the Saladipura pyrite-pyrrhotite deposit and associated rocks, Khetri copper belt, Rajasthan. J. Geol. Soc. India 15, 227–238.

Ray, S.K., 1974b. Inversion of fold-hinge in superposed folding: an example from the Precambrian of central Rajasthan, India. Precambrian Res. 1, 157–164.
Ray, S.K., 1987. Albitite occurrence and associated ore minerals in the Khetri copper belt, Northeastern Rajasthan. Rec. Geol. Surv. India 113, 41–49.
Rino, S., Kon, Y., Sato, W., Maruyama, S., Santosh, M., Zhao, D., 2008. The Grenvillian and Pan-African orogens: world's largest orogenies through geologic time, and their implications on the origin of superplume. Gondwana Res. 14, 51–72.
Rogers, J.J., Santosh, M., 2002. Configuration of Columbia, a Mesoproterozoic supercontinent. Gondwana Res. 5, 5–22.
Roy, A.B., 1995. Geometry and evolution of superposed folding in the Zawar lead-zinc mineralised belt, Rajasthan. Proc. Indian Acad. Sci. Earth Planet Sci. 104, 349–371.
Roy Chowdhury, M.K., Das Gupta, S.P., 1965. Ore-localization in the Khetri copper belt, Rajasthan, India. Econ. Geol. 60, 69–88.
Roy, A.B., Jakhar, S.R., 2002. Geology of Rajasthan (NW India) Precambrian to Recent. Scientific Publishers (India), New Delhi.
Roy, A.B., Nagori, D.K., 1990. Influence of differential basement mobility on contrasting structural styles in the cover rocks: an example from early Precambrian rocks east of Udaipur, Rajasthan. Proc. Indian Acad. Sci. Earth Planet Sci. 99, 291–308.
Roy, A.B., Sharma, K.K., 1999. Geology of the region around Sirohi town, western Rajasthan-a story of Neoproterozoic evolution of the Aravalli crust. In: Paliwal, B.S. (Ed.), Evolution of Northwestern India. Scientific Publishers, Jodhpur, pp. 19–33.
Roy, A.B., Kroner, A., Laul, V., 2001. Detrital zircon constraining basement age in a late Archean greenstone belts of south-eastern Rajasthan. India. Curr. Sci. 81, 407–410.
Roy, A.B., Kroner, A., Rathore, S., Laul, V., Purohit, R., 2012. Tectono-metamorphic and geochronologic studies from Sandmata complex, Northwest Indian Shield: implications on exhumation of Late-Palaeoproterozoic granulites in an Archaean-early Palaeoproterozoic granite-gneiss terrane. J. Geol. Soc. India 79, 323–334.
Roy, A.B., Dutta, K., Rathore, S., 2016. Development of ductile shear zones during diapiric magmatism of nepheline syenite and exhumation of granulites—examples from Central Rajasthan, India. Curr. Sci. 110, 1094–1101.
Ruj, T., Dasgupta, N., 2014. Tectonic imprints within a granite exposed near Srinagar, Rajasthan, India. J. Earth Syst. Sci. 123, 1361–1374.
Sahay, A., Srivastava, D.C., 2005. Ductile shearing along the Great Boundary Fault: an example from the Berach river section, Chittaurgarh Rajasthan. Curr. Sci. 88, 557–560.
Sarkar, S., Biswal, T.K., 2005. Tectonic significance of fissure veins associated with pseudotachylites of the Kui-Chitraseni Shear Zone, Aravalli Mountain, NW India. Gondwana Res. 8, 277–282.
Sarkar, S.C., Dasgupta, S., 1980. Geologic setting, genesis and transformation of sulfide deposits in the northern part of Khetri copper belt, Rajasthan, India—an outline. Mineral. Deposita 15, 117–137.
Sarkar, G., Barman, T.R., Corfu, F., 1989. Timing of continental arc-type magmatism in Northwest India: evidence from U-Pb zircon geochronology. J. Geol. 97, 607–612.
Sarkar, D.P., Ando, J.I., Das, K., Chattopadhyay, A., Ghosh, G., Shimizu, K., Ohfuji, H., 2020. Serpentinite enigma of the Rakhabdev lineament in western India: Origin, deformation characterization and tectonic implications. J. Mineral. Petrol. Sci. 115, 216–226.
Saxena, A., Pandit, M.K., 2012. Geochemistry of Hindoli Group Metasediments, SE Aravalli Craton, NW India: Implications for Palaeoweathering and Provenance. J. Geol. Soc. India 79, 267–278.
Schulz, B., 2021. Monazite microstructures and their interpretation in petrochronology. Front. Earth Sci. 9, 241. https://doi.org/10.3389/feart.2021.668566.
Sen, S., 1980. Precambrian stratigraphic sequence in a part of the Aravalli range, Rajasthan: a re-evaluation. Q. J. Geol. Min. Metall. Soc. India 43, 181–211.
Sengupta, S., Ghosh, S.K., 2004. Analysis of transpressional deformation from geometrical evolution of mesoscopic structures from Phulad shear zone, Rajasthan, India. J. Struct. Geol. 26, 1961–1976.
Sharma, R.S., 1988. Patterns of metamorphism in the Precambrian rocks of the Aravalli mountain belt. In: Roy, A.B. (Ed.), Precambrian of the Aravalli Mountains, Rajasthan, India, Geol. Soc. India Mem, vol. 7, pp. 33–75.
Sharma, K.K., 2005. Malani magmatism: an extensional lithospheric tectonic origin. Geol. Soc. Am. Spec. Pap. 388, 463–476.
Sharma, N.K., Biswal, T.K., 2020. Paleostress and fluid pressure analysis of Vein opening using 3D mohr circle from the quartz vein orientation data of the South Delhi Terrane, Ambaji Area, NW India. Geotectonics 54, 97–105.
Sharma, B.L., Chauhan, N.K., Bhu, H., 1988. Structural geometry and deformation history of the early Proterozoic Aravalli rocks from Baglunda, District Udaipur Rajasthan. Geol. Soc. India Mem. 7, 169–191.
Sharma, P., Shandilya, A.K., Srivastave, N., 2020. Geological settings, mineralization and genesis of iron ore deposit at Pur-Banera Belt of District Bhilwara, Rajasthan (India). Int. J. Geoinf. Geol. Sci. 7, 47–54.
Sharma, N.K., Chinnasamy, S.S., Biswal, T.K., 2022. Genesis of the late-stage base metal sulfide mineralization and its relationship with the regional deformation in Ambaji-Deri, South Delhi Terrane, North-West India. Geol. J. (in press).
Singh, S.P., 1988. Sedimentation patterns of the Proterozoic Delhi Supergroup, northeastern Rajasthan, India, and their tectonic implications. Sediment. Geol. 58, 79–94.
Singh, Y.K., De Waele, B., Karmakar, S., Sarkar, S., Biswal, T.K., 2010. Tectonic setting of the Balaram-Kui-Surpagla-Kengora granulites of the South Delhi Terrane of the Aravalli Mobile Belt, NW India and its implication on correlation with the East African Orogen in the Gondwana assembly. Precambrian Res. 183, 669–688.
Singh, S., Shukla, A., Umasankar, B.H., Biswal, T.K., 2020. Timing of South Delhi orogeny: Interpretation from structural fabric and granite Geochronology, Beawar-Rupnagar-Babra area, Rajasthan, NW India. In: Biswal, T.K., et al. (Eds.), Structural Geometry of Mobile Belts of the Indian Subcontinent, Society of Earth Scientists Series. Springer Nature, Switzerland AG, pp. 1–22. https://doi.org/10.1007/978-3-030-40593-9_1.
Singh, S., De Waele, B., Shukla, A., Umasankar, B.H., Biswal, T.K., 2021. Tectonic fabric, geochemistry, and zircon-monazite geochronology as proxies to date an orogeny: example of South Delhi Orogeny, NW India, and implications for East Gondwana tectonics. Front. Earth Sci. 8, 711. https://doi.org/10.3389/feart.2020.594355.
Sinha-Roy, S., 1988. Proterozoic Wilson cycles in Rajasthan. In: Roy, A.B. (Ed.), Precambrian of the Aravalli Mountain, Rajasthan India, Geol. Soc. India Mem, vol. 7, pp. 95–108.
Sinha-Roy, S., 2004. Proterozoic rifting and major unconformities in Rajasthan, and their implications for uranium mineralisation. Explo. Res. Atom. Min. 15, 69–97.
Sinha-Roy, S., Malhotra, G., 1989. Structural relations of Proterozoic cover and its basement: an example from the Jahazpur belt, Rajasthan. J. Geol. Soc. India 34, 233–244.
Sinha-Roy, S., Mohanty, M., Guha, D.B., 1993. Banas dislocation zone in Nathdwara-Khamnor area, Udaipur District, Rajasthan, and its significance on the basement-cover relations in the Aravalli fold belt. Curr. Sci. 65, 68–72.
Sinha-Roy, S., Malhotra, G., Mohanty, M., 1998. Geology of Rajasthan. Geological Society of India, Bangalore.
Sivaraman, T.V., Odom, A.L., 1982. Zircon geochronology of Berach granite of Chittorgarh, Rajasthan. J. Geol. Soc. India 23, 575–577.
Srivastava, D.C., 2001. Deformation pattern in the Precambrian basement around Masuda, central Rajasthan. J. Geol. Soc. India 57, 197–222.
Sugden, T.J., Deb, M., Windley, B.F., 1990. The tectonic setting of mineralisation in the Proterozoic Aravalli-Delhi orogenic belt, NW India. In: N.S.M (Ed.), Precambrian Continental Crust and its Economic Resources. Elsevier, New York, pp. 367–390.
Synchanthavong, S.P., Desai, S.D., 1977. Protoplate tectonics controlling the Precambrian deformation and metallogenic epochs in NW India. Miner. Sci. Eng. 1, 218–236.
Tapponnier, P., Peltzer, G., LeDain, A.Y., Armijo, R., Cobbold, P., 1982. Propagating extrusion tectonics in Asia: New insights from simple experiments with plasticine. Geology 10, 611–616.
Tiwari, S.K., Biswal, T.K., 2019. Dynamics, EPMA Th-U-total Pb monazite geochronology and tectonic implications of deformational fabric in the lower-middle crustal rocks: a case study of Ambaji granulite, NW India. Tectonics 38, 2232–2254.
Tiwari, S.K., Beniest, A., Biswal, T.K., 2020a. Variation in vorticity of flow during exhumation of lower crustal rocks (Neoproterozoic Ambaji granulite, NW India). J. Struct. Geol. 130, 103912 https://doi.org/10.1016/j.jsg.2019.103912.
Tiwari, S.K., Beniest, A., Biswal, T.K., 2020b. Extension driven brittle exhumation of the lower-middle crustal rocks, a paleostress reconstruction of the Neoproterozoic Ambaji Granulite, NW India. J. Asian Earth Sci. 195, 104341 https://doi.org/10.1016/j.jseaes.2020.104341.
Wang, W., Cawood, P.A., Pandit, M.K., Zhou, M., Chen, W., 2017. Zircon U–Pb age and Hf isotope evidence for an Eoarchaean crustal remnant and episodic crustal reworking in response to supercontinent cycles in NW India. J. Geol. Soc. 174, 759–772.
Wiedenbeck, M., Goswami, J.N., 1994. High precision $^{207}Pb/^{206}Pb$ zircon geochronology using a small ion microprobe. Geochim. Cosmochim. Acta 58, 2135–2141.
Yadav, P.K., 2015. Geology of Rajpura-Dariba group of rocks. Int. Res. J. Geol. Min. 2, 89–102.
Zhao, G., Cawood, P.A., Wilde, S.A., Sun, M., 2002. Review of global 2.1–1.8 Ga orogens: implications for a pre-Rodinia supercontinent. Earth-Sci. Rev. 59, 125–162.
Zhao, G., He, Y., Sun, M., 2009. The Xiong'er volcanic belt at the southern margin of the North China Craton: Petrographic and geochemical evidence for its outboard position in the Paleo-Mesoproterozoic Columbia Supercontinent. Gondwana Res. 16, 170–181.
Zhao, J.H., Pandit, M.K., Wang, W., Xia, X.P., 2018. Neoproterozoic tectonothermal evolution of NW India: evidence from geochemistry and geochronology of granitoids. Lithos 316, 330–346.